



**UNIVERSITY OF LEEDS**

This is a repository copy of *Seismic response assessment of architectural non-structural LWS drywall components through experimental tests*.

White Rose Research Online URL for this paper:  
<http://eprints.whiterose.ac.uk/141729/>

Version: Accepted Version

---

**Article:**

Landolfo, R, Pali, T, Bucciero, B et al. (5 more authors) (2019) Seismic response assessment of architectural non-structural LWS drywall components through experimental tests. *Journal of Constructional Steel Research*, 162. 105575. ISSN 0143-974X

<https://doi.org/10.1016/j.jcsr.2019.04.011>

---

© 2019, Elsevier. This manuscript version is made available under the CC-BY-NC-ND 4.0 license <http://creativecommons.org/licenses/by-nc-nd/4.0/>.

**Reuse**

This article is distributed under the terms of the Creative Commons Attribution-NonCommercial-NoDerivs (CC BY-NC-ND) licence. This licence only allows you to download this work and share it with others as long as you credit the authors, but you can't change the article in any way or use it commercially. More information and the full terms of the licence here: <https://creativecommons.org/licenses/>

**Takedown**

If you consider content in White Rose Research Online to be in breach of UK law, please notify us by emailing [eprints@whiterose.ac.uk](mailto:eprints@whiterose.ac.uk) including the URL of the record and the reason for the withdrawal request.



[eprints@whiterose.ac.uk](mailto:eprints@whiterose.ac.uk)  
<https://eprints.whiterose.ac.uk/>

# SEISMIC RESPONSE ASSESSMENT OF ARCHITECTURAL NON-STRUCTURAL LWS DRYWALL COMPONENTS THROUGH EXPERIMENTAL TESTS

Landolfo Raffaele\*

*Department of Structures for Engineering and Architecture, University of Naples "Federico II", Naples, Italy,*  
landolfo@unina.it

Pali Tatiana

*Department of Structures for Engineering and Architecture, University of Naples "Federico II", Naples, Italy,*  
tatiana.pali@unina.it

Bucciero Bianca

*Department of Structures for Engineering and Architecture, University of Naples "Federico II", Naples, Italy,*  
bianca.bucciero@unina.it

Terracciano Maria Teresa

*Department of Structures for Engineering and Architecture, University of Naples "Federico II", Naples, Italy,*  
mariateresa.terracciano@unina.it

Shakeel Sarmad

*Department of Structures for Engineering and Architecture, University of Naples "Federico II", Naples, Italy,*  
sarmad.shakeel@unina.it

Macillo Vincenzo

*Department of Structures for Engineering and Architecture, University of Naples "Federico II", Naples, Italy,*  
vincenzo.macillo@unina.it

Iuorio Ornella

*School of Civil Engineering, University of Leeds, Leeds, United Kingdom, o.iuorio@leeds.ac.uk*

Fiorino Luigi

*Department of Structures for Engineering and Architecture, University of Naples "Federico II", Naples, Italy,*  
lfiorino@unina.it

\*Corresponding Author: Department of Structures for Engineering and Architecture, University of Naples "Federico II", Via Forno Vecchio 36, 80134 Naples, ITALY; Phone: +39 081 2538052; Fax: +39 081 2538989

**Keywords:** indoor partition walls; in-plane and out-of-plane tests; lightweight steel; outdoor façade walls; shake table tests; suspended ceilings.

## ABSTRACT

A research project was conducted at University of Naples "Federico II" over the last few years with the aim to give a contribute to overcome the lack of information on seismic behaviour of architectural

non-structural lightweight steel (LWS) drywall components, i.e. indoor partition walls, outdoor façades and suspended continuous ceilings. The tested non-structural components were made of LWS frames sheathed with gypsum-based or cement-based boards. The research activity was organized in three levels: ancilliary tests, component tests and assembly tests. Ancilliary tests were carried out for evaluating the local behaviour of partitions, façades and ceilings. Component tests involved out-of-plane quasi-static monotonic and dynamic identification tests and in-plane quasi-static reversed cyclic tests on partitions. Finally, the dynamic behaviour was investigated through shake table tests on different assemblages of partitions, façades and ceilings. The study demonstrated that the tested architectural non-structural LWS drywall components are able to exhibit a very good seismic behaviour with respect to the damage limit states according to the IDR limits given by Eurocode 8 Part 1. The current paper describes the complete experimental activity within the project.

## **1. INTRODUCTION**

The lack of understanding on the seismic behaviour of architectural non-structural components is becoming one of the most important issue of the structural design within the framework of performance based-design. The interest about this aspect was boosted further in recent years among research teams and industrial entities after the occurrence of some major seismic events (1964 Alaska earthquake, 1971 San Fernando earthquake, 1989 Loma Pietra earthquake, 1994 Northridge earthquake, 1995 Kobe earthquake, 2009 L’Aquila earthquake, 2010 Chile earthquake, 2012 Emilia earthquake). During these earthquakes, damages were detected in architectural non-structural components and some important consequences were highlighted in terms of economical, functional and human life losses. In particular, these consequences acquired more importance in the case of schools, hospital, museums and other strategic buildings. Furthermore, taking into account the substantial initial investment that is associated with the installation of architectural non-structural components in the most commonly used buildings, it appears clear that the damages of these components represented a substantial property economic loss. In this context, the main aim of the current researches and codifications [1-3] is the introduction of specific design requirements in terms of strength and deformation for architectural non-structural components in order to ensure collapse prevention and to reduce the seismic vulnerabilities by imposing limits for the damage limitation control.

The current work intends to deepen the seismic behaviour of architectural non-structural lightweight steel (LWS) drywall components, i.e. indoor partition walls, outdoor façades and suspended continuous ceilings, named in the following simply partitions, façades and ceilings, respectively. The motivations that direct the interest on this topic are related to the ever-increasing diffusion of these systems in the current construction market. The growing spread of these systems is essentially due to

their ability to ensure appropriate environmental, economic and seismic performances, which make them very innovative and competitive constructional systems compared to traditional systems in seismic and non-seismic areas. In particular, the knowledge and prediction of the seismic performance represents a complex issue that could be investigated through experimental activities. Indeed, over the last few years, along with several studies on architectural non-structural LWS drywall components, which were mainly focused on fire behaviour [4-5], effect on the structural response [6-11], joining technologies [12-13], diaphragm action [14-15] and behaviour under axial and lateral loads [16-17], a large number of research studies were also undertaken on investigating the seismic behaviour. Generally, these researches included the study of the local and global behaviour: seismic behaviour of board-to-frame fixings adopted for realizing partitions and façades [18-21]; seismic behaviour under monotonic, quasi-static cyclic and dynamic loadings in the in-plane [22-34] and out-of-plane [35-36] directions of partitions and façades; study of the interaction between partitions and façades and/or ceilings and surrounding elements by means of shake table tests on full-scale one or multi-storeys buildings completed with architectural non-structural components [37-45]. In particular, the main aims of the cited research studies were to provide information about the seismic behaviour of architectural non-structural components by investigating the following aspects: (i) damageability and seismic fragilities ([25], [30-31], [34], [37-41], [44-45]); (ii) mechanical response under monotonic [36], cyclic ([23], [25-26], [31] and [34]) and dynamic loading ([23], [35], [37-45]); (iii) effect of the constructional details on the seismic response, i.e. stud dimensions and spacing ([25], [27], [30-31] and [34]), presence of back-to-back studs [31-32], track dimensions [31], board thickness, type, number and orientation ([22], [25], [27], [31] and [34]), board-to-frame fixing type and spacing ([24], [25], [27], [31-32]), wall finishing type ([24] and [34]), presence of doors or windows ([22-23] and [25]), partial-height partitions [30], aspect ratio of partitions [27], presence of damper devices [33]; (iv) effect of the loading conditions (quasi-static or dynamic) on the lateral response ([23-24], [27] and [30]); (v) estimation of the repair costs after a seismic event ([23], [28] and [34]); (vi) interaction with surrounding elements ([22], [34], [38], [39], [40] and [45]); (vii) evaluation of dynamic amplification and dynamic parameters [43-45]; (viii) presence of mechanical and electrical non-structural components [41] and building furnishing and contents [35].

Therefore, a relatively large database of experimental results is available, but several specific issues still require further investigation, such as: mechanical behaviour of steel material, screws and sheathing boards adopted for realizing partitions, façades and ceilings; seismic behaviour of board-to-frame fixings adopted for realizing partitions and façades; out-of-plane seismic behaviour of partitions; seismic behaviour of façades; seismic behaviour of several non-structural components interacting with surrounding elements; estimation of the required repair costs for partitions and façades after a seismic event. In order to provide additional information about the assessment of these

several aspects, an extended research activity was performed at the Laboratory of the Department of Structures for Engineering and Architecture at the University of Naples “Federico II”. In particular, the research project focused on the assessment of the performance of architectural non-structural LWS drywall components, i.e. partitions, façades and ceilings, under seismic actions. This paper presents the whole experimental activity. Information about the tested non-structural components, test plan, out-of-plane tests, in-plane tests, shake table tests and seismic fragility evaluation is provided in the following sections.

## **2. EXPERIMENTAL PROGRAM**

### **2.1. Tested non-structural components**

The focus of the experimental research was the assessment of the seismic behaviour of architectural non-structural LWS drywall components, i.e. partitions, façades and ceilings. The tested non-structural components were made of LWS frames made with the adoption of cold-formed steel (CFS) profiles and sheathed with gypsum-based or cement-based boards. All basic components were dry assembled. In particular, the interaction between partitions and surrounding elements and/or façades and ceilings was taken into account during the experimental activity. To this end, four cases of practical application of architectural non-structural LWS drywall components installed in a surrounding structure, i.e. reinforced concrete structure, were considered (Fig. 1): (a) Case A, in which partition interacted with structural elements; (b) Case B, in which partition interacted with both structural and non-structural elements; (c) Case C, in which façade interacted with structural elements; (d) Case D, in which ceiling interacted with non-structural elements. Therefore, four architectural non-structural LWS drywall components representative of the corresponding cases of application were identified: (1) Component 1 representing Case A, in which partition was infilled in the surrounding structure and enclosed by structural elements on all sides (i.e. floors or beams and columns); (2) Component 2 representing Case B, in which partition was enclosed by structural elements at the top and bottom (i.e. floors or beams) and connected at its ends to transversal façades (return walls); (3) Component 3 representing Case C, in which façade was infilled in the surrounding structure and enclosed by structural elements on all sides (i.e. floors or beams and columns); (4) Component 4 representing Case D, in which ceiling was suspended from the above floors and connected at the perimeter to partitions and façades.

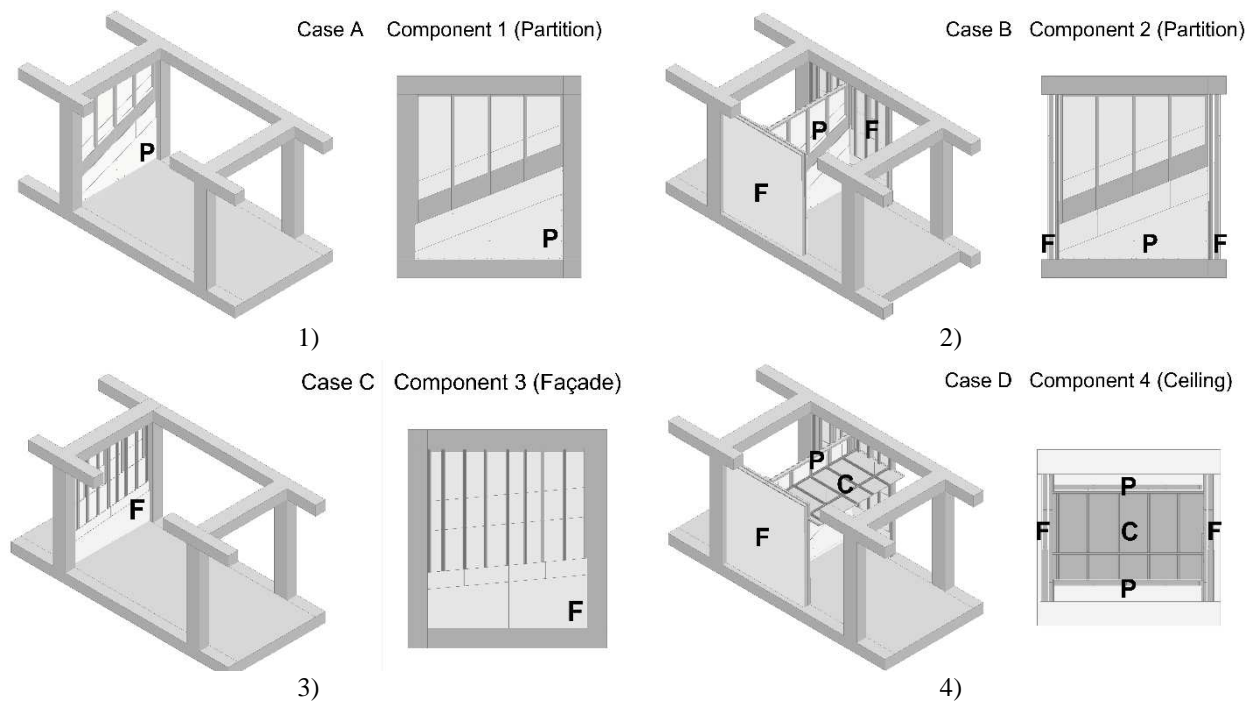


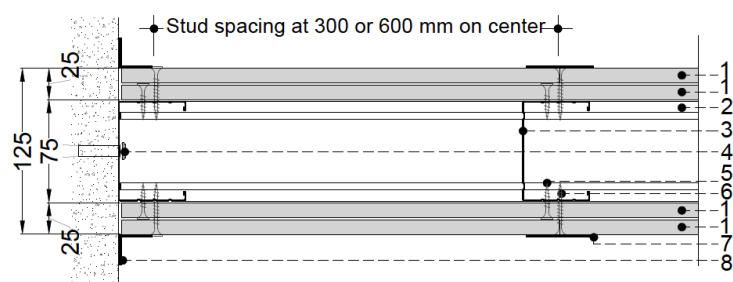
**Fig. 1.** Practical applications (cases A to D) and relevant architectural non-structural LWS drywall components (Components 1 to 4); P: Partition; F: Façade; C: Ceiling

The tested partitions were made of a single LWS frame sheathed with gypsum-based panels (Fig. 2). The steel frame was made with lipped channel section stud profiles ( $75 \times 50 \times 7.5 \times 0.6$  mm, outside-to-outside web depth  $\times$  outside-to-outside flange size  $\times$  outside-to-outside lip size  $\times$  thickness) spaced at 300 or 600 mm on centre and connected at the ends to unlipped channel section track profiles ( $75 \times 40 \times 0.6$  mm, outside-to-outside web depth  $\times$  outside-to-outside flange size  $\times$  thickness). The steel frame was completed with double layer of 12.5 mm thick standard gypsum (GWB) or gypsum-fibre (GFB) boards installed on both partition faces. The board-to-frame fixings were realized with 3.5 mm nominal diameter self-piercing screws spaced from 250 to 700 mm on centre, whereas the partition-to-surrounding fixings were made with 6 mm (or 8 mm) drilled hole diameter steel or plastic dowels spaced from 500 to 900 mm on centre. Partitions were finished with paper tape (or, in one test, glass fibre tape with alkaline-resistant coating) fixed with gypsum-based plaster for field joints, i.e. joints between adjacent boards, and self-adhesive paper tape (or, in one test, glass fibre tape with alkaline-resistant coating fixed with gypsum-based plaster) for perimeter joints, i.e. joints between partitions and surrounding elements. The total partition thickness was equal to 125 mm.

The façades (Fig. 3) were realized with double LWS frames, i.e. interior and exterior frames. The interior and exterior frames were made of stud profiles ( $50 \times 50 \times 7.5 \times 0.6$  mm spaced at 300 or 600 mm and  $75 \times 50 \times 7.5 \times 0.8$  mm spaced at 600 mm, respectively) connected to track profiles ( $50 \times 40 \times 0.6$  mm and  $75 \times 40 \times 0.8$  mm, respectively). The interior frame was sheathed with two layers of 12.5 mm thick GWB and impact resistant gypsum boards (RGWB) installed on the outer frame

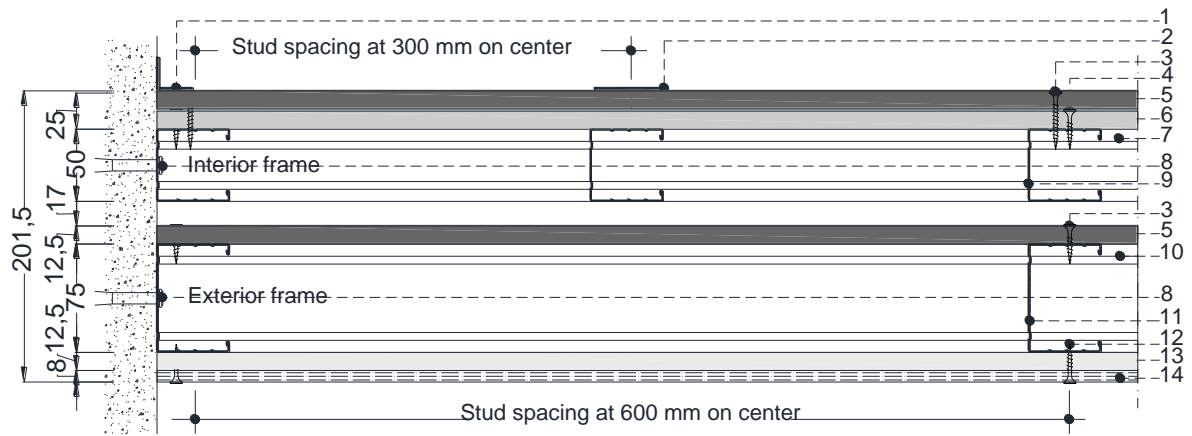
face, whereas 12.5 mm thick RGWB and outdoor cement boards (CP) were placed at the inner and outer face of the exterior frame, respectively. The board-to-frame fixings were realized with self-piercing screws with nominal diameter ranging from 3.5 to 4.2 mm spaced from 200 to 700 mm on centre, whereas the façade-to-surrounding fixings were made with 6 mm (or 8 mm) drilled hole diameter plastic dowels spaced from 500 to 600 mm on centre. The outer face of the interior frame was finished with paper tape fixed with gypsum-based plaster for field joints and with self-adhesive paper tape for perimeter joints. The outer face of the exterior frame was finished with glass fibre tape with alkaline-resistant coating fixed with cement-based plaster for field joints and the whole façade surface was completed with glass fibre tape with an alkaline-resistant coating and cement-based plaster. The total façade thickness was equal to 201.5 mm.

The ceilings (Fig. 4) were made of a double level of LWS profiles, i.e. upper carrying profiles spaced at 1000 mm on centre and connected with metallic clips to transversal lower furring profiles spaced at 500 mm on centre. Both carrying and furring profiles, having lipped channel sections (50×27×7.5×0.6 mm), were connected at the ends of track profiles (27×30×0.6 mm) by means of 4.2 nominal diameter self-tapping screws. Carrying profiles were placed at a distance equal to 500 mm from the floor by means of variable adjustable suspenders. The steel frame was completed at the bottom face with a single layer of 12.5 mm thick sound shield boards (SSB), whereas the board-to-frame fixings and the fixings at the ceiling perimeter were made by means of 3.5 mm nominal diameter self-piercing screws spaced at 200 and 250 mm on centre, respectively. Field joints between adjacent boards were completed with paper tape fixed with gypsum-based plaster, whereas the perimeter joints were finished with self-adhesive paper tape. The total ceiling thickness was equal to 68.6 mm.



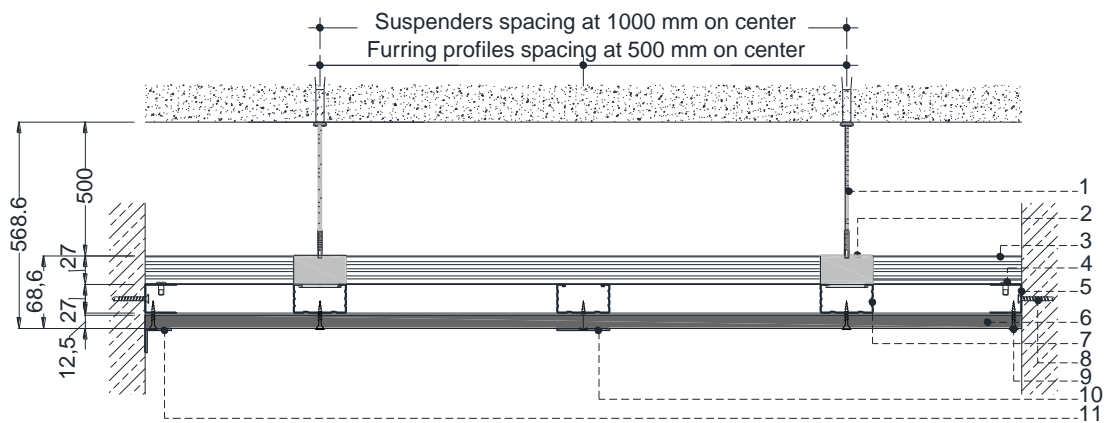
1. 12.5 mm thick standard gypsum or gypsum fibre boards
2. Track profile (75x40x0.6 mm)
3. Stud profile (75x50x7.5x0.6 mm)
4. 6 mm (or 8 mm) drilling hole diameter steel or plastic dowel spaced from 500 to 900 mm
5. 3.5 mm nominal diameter self-piercing screws spaced at 700 mm
6. 3.5 mm nominal diameter self-piercing screws spaced at 250 mm
7. Paper tape (or, in one test, glass fibre tape with alkaline-resistant coating) fixed with gypsum-based plaster
8. Self-adhesive paper tape (or, in one test, glass fibre tape fixed with gypsum-based plaster)

**Fig. 2.** Horizontal section of the tested partitions (lengths in mm)



1. Self-adhesive paper tape
2. Paper tape fixed with gypsum-based plaster
3. 3.9 mm nominal diameter self-piercing screws spaced at 250 mm
4. 3.5 mm nominal diameter self-piercing screws spaced at 700 mm
5. 12.5 mm thick impact resistant gypsum board
6. 12.5 mm thick standard gypsum board
7. Track profile (50x40x0.6 mm)
8. 6 mm (or 8 mm) drilling hole diameter plastic dowel spaced from 500 to 600 mm
9. Stud profile (50x50x7.5x0.6 mm) spaced at 300 mm
10. Track profile (75x40x0.8 mm)
11. Stud profile (75x50x7.5x0.8 mm) spaced at 600 mm
12. 4.2 mm nominal diameter self-drilling screws spaced at 200 mm
13. 12.5 mm thick outdoor cement board
14. Glass fibre tape with alkaline-resistant coating fixed with cement-based plaster

**Fig. 3.** Horizontal section of the tested façades (lengths in mm)

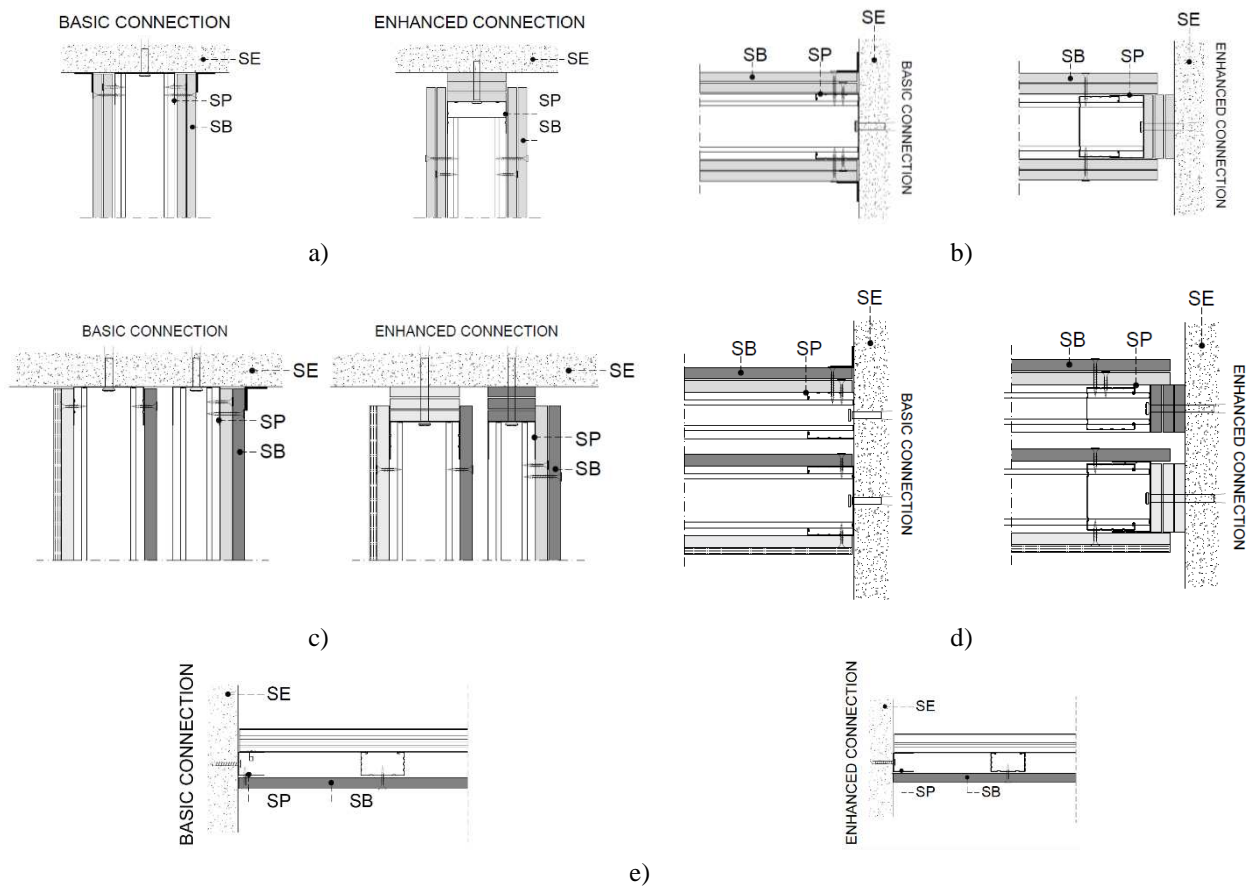


1. Variable adjustable suspender
2. Metallic clip
3. Carrying profile (50x27x7.5x0.6 mm)
4. 4.2 mm nominal diameter self-tapping screw
5. Track profile (27x30x0.6 mm)
6. 12.5 mm thick sound shield board
7. Furring profile (50x27x7.5x0.6 mm)
8. 3.5 mm nominal diameter self-piercing screw spaced at 250 mm
9. 3.5 mm nominal diameter self-piercing screw spaced at 200 mm
10. Paper tape fixed with gypsum-based plaster
11. Self-adhesive paper tape

**Fig. 4.** Vertical section of the tested ceilings (lengths in mm)

All LWS profiles were fabricated with DX51D+Z steel grade for which EN 1993 Part 1-3 [46] provides the nominal minimum values for the yield strength and ultimate tensile strength equal to 140 MPa and 270 MPa, respectively. Furthermore, a range from 270 to 500 MPa for the nominal ultimate tensile strength is given by EN 10346 [47].

Tested non-structural components were connected to both structural and non-structural surrounding elements by means of two different typologies of connections: basic and enhanced anti-earthquake connections. The relative displacements between non-structural components and surrounding elements were restrained in the case of basic connections, whereas the in-plane displacements were allowed in the case of enhanced anti-earthquake connections. In particular, the enhanced anti-earthquake connections allowed the sliding of non-structural components respect to the surrounding elements in such a way to isolate them from the building deformations in the case of seismic events. Specifically, basic connections were made by fixing sheathing boards to surrounding profiles, whereas surrounding profiles and sheathing boards were not connected in the case of enhanced anti-earthquake connections. Furthermore, the enhanced anti-earthquake connections were located at the top (i.e. horizontal connections between partitions or façades and floors or beams) and/or lateral sides (i.e. vertical connections between partitions or façades and columns) of partitions and façades and at the ceiling perimeter. Only in the case of partitions and façades, a gap between sheathing boards and surrounding elements was used. Fig. 5 shows the adopted connection typologies for partitions (Fig. 5a and b), façades (Fig. 5c and d) and ceilings (Fig. 5e).



SE: surrounding element; SB: sheathing board; SP: surrounding profile

**Fig. 5.** Connections adopted between the tested non-structural components and surrounding elements: a) horizontal connections for partitions; b) vertical connections for partitions; c) horizontal connections for façades; d) vertical connections for façades; e) vertical connections for ceilings

## 2.2. Test plan

A wide experimental campaign was carried out for evaluating the seismic behaviour of partitions, façades and ceilings. With the aim of having a broad vision of the local and global response of the tested components, the research activity was organized in three levels: ancilliary tests, component tests and assembly tests. The attempt of ancilliary tests was to characterize the mechanical behaviour of steel material, screws, sheathing boards and board-to-frame fixings, which strongly affected the global response of partitions, façades and ceilings. More data about the ancilliary tests are provided in [18].

Component tests were performed on full-scale partitions for assessing the out-of-plane and in-plane behaviour. The goal was to provide answers to the prescriptions for out-of-plane and in-plane design of partitions according to Eurocode 8. The procedure for evaluating the seismic demand on acceleration-sensitive components (out-of-plane design) by means of the equivalent static design force method is given in Eurocode 8 Part 1 Section 4.3.5, whereas the design criteria for defining the

relative displacement seismic demand on deformation-sensitive components (in-plane design) by imposing inter-storey drift limits are provided in Eurocode 8 Part 1 Section 4.4.3.

As far as the out-plane design of partitions is concerned, the main unknown variables, which play a significant role in the seismic verification of acceleration-sensitive components, to be estimated are the out-of-plane design resisting force and the fundamental vibration period. However, Eurocode 8 does not provide criteria for evaluating the design resisting force, which could be evaluated experimentally or with analytical methods. Therefore, three-point bending tests under quasi-static monotonic loads were performed in the out-of-plane direction of full-scale partitions for evaluating the wall design resisting force. This experimental activity was limited to monotonic tests, but a more proper evaluation of the out-of-plane design resisting force should be carried out in cyclic loading regime. In particular, three-point bending tests were adopted according to the structural model of partitions provided by Eurocode 8. In fact, the codified seismic verification of acceleration-sensitive components requires that the design resisting force is compared with the design seismic force applied at the component's centre of mass in the most unfavourable direction, i.e. out-of-plane direction. Furthermore, the design seismic force depends by several parameters, but the main unknown parameter is the fundamental vibration period for which usually no information is available in literature. Therefore, out-of-plane dynamic identification tests, namely step-relaxation tests, were carried out for defining the fundamental vibration period. Specifically, out-of-plane quasi-static monotonic and dynamic identification tests were performed on Component 1. More information about out-of-plane tests is provided in [36].

As far as the in-plane behaviour is concerned, the seismic verification of deformation-sensitive components defined according to Eurocode 8 requires that the non-structural components should satisfy the damage limitation requirement obtained by limiting the design inter-storey drifts of the main structure to the code-specific values. Specifically, EN 1998 requires that the inter-storey drift ratio (IDRs), defined as the ratio between the design inter-storey drift corrected with a reduction factor and the storey height, should be limited to: 0.5 % for buildings having non-structural components made of brittle materials and attached to the structure; 0.75 % for buildings having ductile non-structural components; 1.0 % for buildings having ductile non-structural components fixed in a way so as not to interfere with structural deformations. Therefore, in-plane quasi-static reversed cyclic test were performed for investigating the damages and the seismic fragilities of partitions. The main aim was to elaborate seismic fragility curves to be compare with the inter-storey drift limits defined by Eurocode 8. In particular, in-plane quasi-static reversed cyclic tests were conducted on Components 1 and 2 [34].

Finally, the dynamic behaviour was estimated by means of shake table tests, which were carried out for evaluating the out-of-plane behaviour of partitions and the in-plane behaviour of partitions,

façades and ceilings. In particular, shake table tests were performed on different assemblages of Components 1, 2, 3 and 4 [45]. In this study, the effect of the interaction between out-of-plane and in-plane actions on components was neglected. However, the interaction between the out-of-plane and in-plane behaviour of partitions was evaluated by several researches through bidirectional shake table tests on non-structural components [39] [44], but specific conclusions about the effect of the interaction are not given.

Table 1 summarizes the matrix for component and assembly tests.

**Table 1.** Test matrix

Test type		Component	Direction of the seismic action <sup>(1)</sup>	No. of tests	
Component tests		Out-of-plane quasi-static monotonic tests	1	Out-of-plane	22
		Out-of-plane dynamic identification tests	1	Out-of-plane	11
		In-plane quasi-static reversed cyclic tests	1	In-plane	8
			2	In-plane	4
Assembly tests	Shake table tests		1	Out-of-plane, in-plane	5
			2	Out-of-plane	
			3	In-plane	
			4	In-plane	
				Total no. of tests	

<sup>(1)</sup> Direction of the seismic action respect to the plane of the component

### 3. OUT-OF-PLANE TESTS

#### 3.1. Quasi-static monotonic tests

Out-of-plane quasi-static monotonic tests were performed with the main aim to identify the out-of-plane behaviour of partitions in terms of strength, stiffness and damage phenomena. In particular, three-point bending tests under quasi-static monotonic loads were carried out on the Component 1 (Fig. 6). Two typologies of partitions (Component 1) were tested: (1) 1800 mm long and 2700 mm high walls, named “tall partitions”; and (2) 1800 mm long and 600 mm high walls, named “short partitions”. The height of “tall partition” walls was selected considering the most common European applications of partitions, whereas the height of “short partition” walls was set equal to 600 mm, which represents the maximum height for inducing the collapse of the partition-to-surrounding connections. The main objectives of tests on “tall partitions” were to investigate the damage phenomena and evaluate the out-of-plane strength and fundamental vibration period that are required by the seismic verification of acceleration-sensitive components according to Eurocode 8 Part 1 - Section 4.3.5. The main goals of tests on “short partitions” were to induce the collapse of the partition-to-surrounding connections and to identify the out-of-plane behaviour and damage phenomena of connections.



**Fig. 6.** Out-of-plane quasi-static monotonic tests on “tall partitions”

Test program was organized in order to investigate the following parameters: (1) Partition height (600 or 2700 mm); (2) stud spacing (300 or 600 mm); (3) types of partition-to-surrounding connections, (basic or enhanced anti-earthquake connections) for realizing the horizontal connections between partitions and top and bottom beams; (4) dowel types for realizing the partition-to-surrounding fixings, i.e. plastic or steel; (5) gap between sheathing boards and surrounding elements, i.e. 20 or 30 mm for enhanced anti-earthquake connections. A total number of 14 and 8 tests were carried out on “tall” and “short” partitions, respectively. Table 2 shows the test matrix for out-of-plane monotonic tests. Only results obtained for “tall partitions” are illustrated in this paper, whereas further information about tests of “short partitions” can be found in [29].

The tests were performed by adopting a specific test set-up designed for applying the monotonic load in the out-of-plane direction at the mid-span of partitions arranged in horizontal position (Fig. 7). The test set-up consisted of two reinforced concrete structures, which supported the partitions by means of a steel supporting system made of S275JR steel grade hot-rolled profiles. The load was transferred by a hydraulic actuator to the bottom face of partition by means of two beams arranged in direction parallel to the partition length and connected each to other through fixed restraint systems, i.e. threaded bars. For simulating the interface of a reinforced concrete structure, C25/30 strength class 50 mm thick concrete blocks were interposed between the tested partitions and the steel supporting system. The adopted instrumentation consisted of 8 potentiometers placed on both partition sides for measuring the vertical displacements at the supports and mid-span. Specimens were subjected to progressive displacements up to failure under a displacement-controlled procedure.

**Table 2.** Test matrix for out-of-plane quasi-static monotonic tests

Component	Specimen label	Partition height [mm]	Stud spacing [mm]	Horizontal connections <sup>(1)</sup>		Dowel types <sup>(2)</sup>	Gap <sup>(3)</sup>	No. of tests
				top	bottom		top	
<b>“tall partition”</b>								
1	#1, #2, #3	2700	600	B	B	P	0	3
1	#4	2700	300	B	B	P	0	1
1	#5	2700	300	B	B	P	0	1
1	#6, #7	2700	600	B	B	S	0	2
1	#8	2700	300	B	B	S	0	1
1	#9	2700	600	E	B	P	30	1
1	#10,#11,#12	2700	600	E	B	P	20	3
1	#13	2700	600	E	B	S	30	1
1	#14	2700	600	E	B	S	20	1
Total no. of tests								14
<b>“short partition”</b>								
1	#15, #16	600	600	B	B	P	0	2
1	#17, #18	600	600	B	B	S	0	2
1	#19	600	600	E	B	P	30	1
1	#20	600	600	E	B	P	20	1
1	#21	600	600	E	B	S	30	1
1	#22	600	600	E	B	S	20	1
Total no. of tests								8

<sup>(1)</sup> Horizontal connections between partitions and top and bottom beams (representing the connections between partitions and floors or beams); B: basic connections, E: enhanced anti-earthquake connections.

<sup>(2)</sup> Dowel types; P: plastic dowel, S: steel dowels.

<sup>(3)</sup> Gap between sheathing boards and surrounding elements.

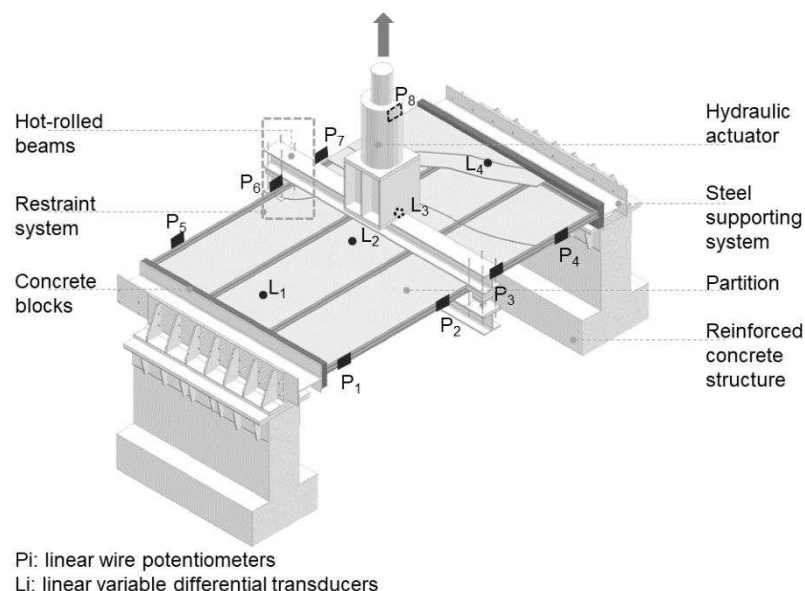


**Fig. 7.** Test set-up and adopted instrumentation

The parameters used to describe the experimental behaviour were defined on the load (F) versus displacement (d) curves, in which d was the displacement recorded by the four potentiometers placed

at wall mid-span. The response curves obtained by monotonic tests on “tall partitions” are shown in Fig. 8. The partitions showed a behaviour initially characterized by an increasing trend of the load as the displacement increased until the first-peak load was reached. After that, a softening behaviour followed by a load increasing up to the second-peak load was observed and the load reduction was detected at the end of tests. The defined parameters were the first-peak strength ( $F_{1st}$ ), the second-peak strength ( $F_{2nd}$ ) and the conventional elastic stiffness ( $k_e$ ), which was assumed equal to the ratio between the conventional elastic limit load equal to  $0.4F_{1st}$  and the relevant displacement.

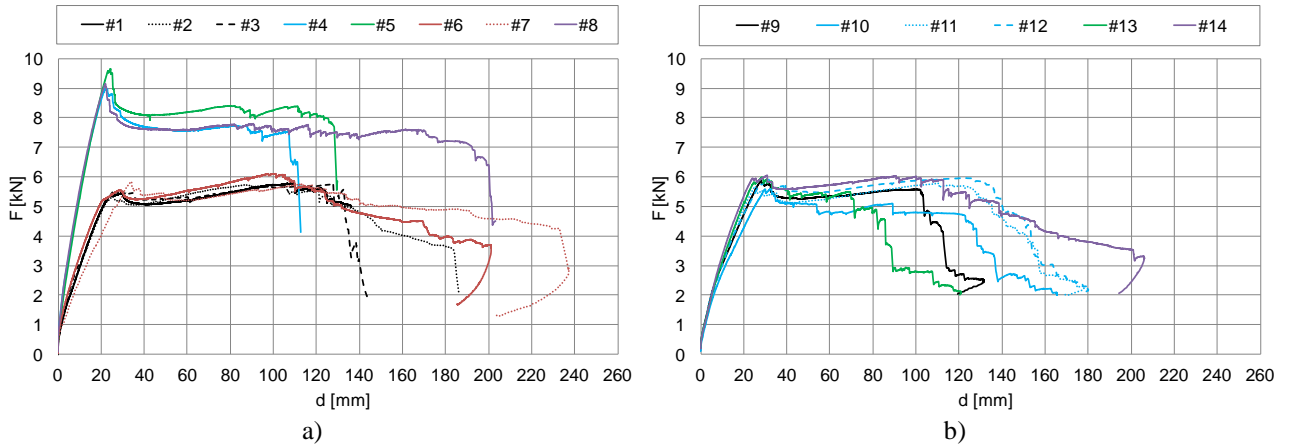


**Fig. 8.** Response curves for out-of-plane quasi-static monotonic tests on: (a) “tall partitions” with basic connections; (b) “tall partitions” with enhanced anti-earthquake connections.

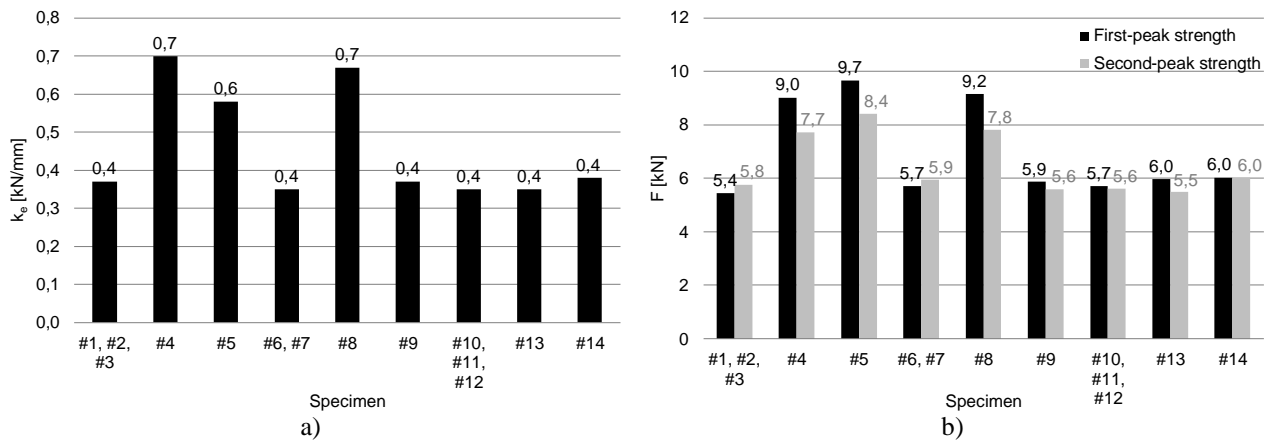


**Fig. 9.** Values of main parameters for “tall partitions”: a) conventional elastic stiffness; b) strength.

Furthermore, the static fundamental vibration frequency  $f_s$  of the tested partition walls was theoretically evaluated by monotonic test data. In particular, the structural scheme of a simple supported beam with distributed mass was adopted for the tested partition walls and the static fundamental vibration frequency was estimated with the well-known following relationship [48]:

$$f_s = \left(\frac{n}{h}\right)^2 \cdot \frac{\pi}{2} \cdot \sqrt{\frac{EI}{\rho}} \quad (1)$$

in which  $n$  is the wall eigenmodes number, set equal to 1;  $h$  is the wall height, set equal to 2700 mm;  $EI$  is the wall bending stiffness, defined on the linear branch of the obtained experimental load  $F$  vs.

displacement  $d$  curve;  $\rho$  is the wall linear density, defined as the ratio between the total wall mass and the wall height.

Physical phenomena related to the wall framing local buckling generally characterized the initial behaviour of the tested walls and, in particular, stud local buckling (Fig. 10a) was observed at the first-peak load, whereas the second-peak load was reached when flexural cracking of sheathing boards occurred (Fig. 10b). Test results and average values for configurations with more nominally identical specimens are presented in Fig. 9 in terms of conventional elastic stiffness and strength. The results show that the initial response was affected by the stud spacing, which produced a strongly increment of the conventional elastic stiffness and strength when spacing passing from 600 to 300 mm. In particular, test results show that 300 mm stud spacing partitions, #4, #5 and #8, exhibited doubled values of conventional elastic stiffness (from 0.6 to 0.7 kN/mm) and strength (from 9.0 to 9.7 kN for the first-peak strength and from 7.7 to 8.4 kN for the second-peak strength) compared to 600 mm stud spacing partitions, #1, #2, #3, #6, #7, #9, #10, #11, #12, #13 and #14 (about 0.4 kN/mm for stiffness and from 5.4 to 6.0 kN for the first-peak strength and from 5.5 to 6.0 kN for the second-peak strength). The advanced post-second peak response phase was strongly influenced by the partition-to-surrounding connection types (basic or enhanced anti-earthquake connections, as described in Section 2.1 and showed in Fig. 5). Basic-connection partitions, #1, #2, #3, #6 and #7, showed a residual load capacity after the post-second peak response due to the membrane behaviour emerging for higher out-of-plane deflections (Fig. 8a), whereas enhanced-connection partitions, #9, #10, #11, #12, #13 and #14, exhibited a more brittle post-second peak response with a lower membrane residual load capacity due to the lower extensional restrain effect provided by the supports (Fig. 8b). Furthermore, dowel types affected the post-second peak response and phenomena related to the connection collapse occurred, i.e. dowel pull-out from the concrete supports (Fig. 10c) and failure of the board-to-frame fixings at the partition supports (Fig. 10d) in the case of basic-connection partitions with plastic and steel dowels, respectively, and stud-to-track detachment (Fig. 10e) in the case of enhanced-connection partitions. The experimental values of the out-of-plane resistance were compared with the theoretical values obtained by means of the effective width method (EWM) according to EN 1993 Part 1-3 in Section 5.5 and the direct strength method (DSM) illustrated in Appendix 1 of AISI S100-16 [49]. Both method overestimated the experimental strength, but the predicted values provided by EWM (average overestimation of 16%) were better than those obtained with DSM (average overestimation of 55%). Further information about the out-of-plane quasi-static monotonic tests can be found in [36].

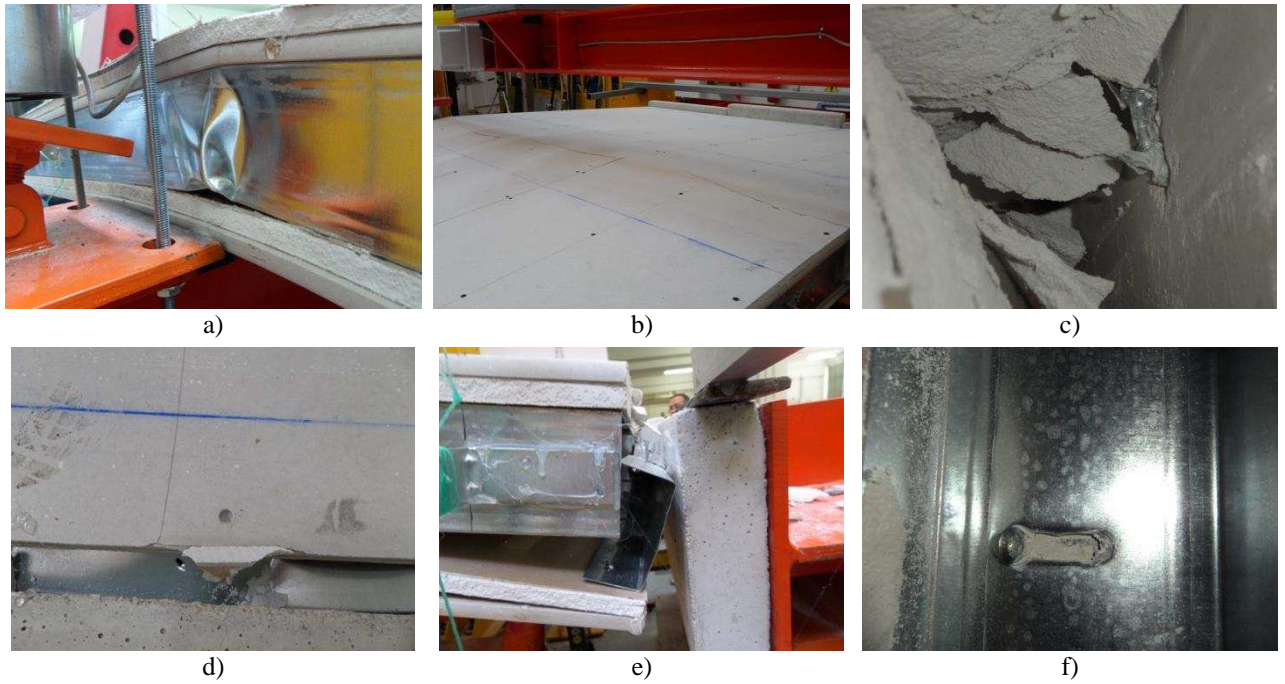


**Fig. 10.** Observed damage phenomena

### 3.2. Dynamic identification tests

Out-of-plane dynamic identification tests were carried out only on “tall partitions” in order to experimentally quantify the fundamental vibration frequency and damping ratio. The parameters under investigation are the same described for out-of-plane quasi-static monotonic tests and summarized in Table 3. A total number of 11 tests were carried out on “tall partitions”.

The tests were performed by adopting the same test set-up designed for out-of-plane quasi-static monotonic tests and described in the previous section, with few changes. The restraint system between the upper and lower beams of test set-up, in the case of dynamic tests, was made of electromagnetic devices, which were deactivated to a given load/displacement value by releasing the lower beam and allowing the free vibration of the wall. In particular, the adopted electromagnetic device had a maximum nominal load capacity of 3.0 kN. As far as the instrumentation is concerned, 4 linear variable differential transducers (LVDTs) were adopted for measuring the free vibration of partitions in vertical direction at the supports ( $L_1$  and  $L_4$  in Fig. 7) and mid-span ( $L_2$  and  $L_3$ ). The dynamic identification was carried out through step-relaxation tests, i.e. specimens were subjected to progressive quasi-static loads until a load of 2.0 kN was obtained and then the load is suddenly released.

Dynamic identification tests provided the displacement ( $d$ ) versus time ( $t$ ) curves (Fig. 11), in which the displacement was recorded by the LVDTs placed at the mid-span of the partition. Test results and the average values for configurations with more nominally identical specimens are presented in Fig. 12 in terms of damping ratio ( $\zeta$ ) and experimental fundamental vibration frequency ( $f_D$ ) together with the values of the static (theoretical) fundamental vibration frequency  $f_s$  obtained according to

Equation (1). Specifically, the logarithmic decay method was adopted for evaluating damping ratio and fundamental vibration frequency.

**Table 3.** Test matrix for out-of-plane dynamic identification tests

Component	Specimen label	Partition height [mm]	Stud spacing [mm]	Horizontal connections <sup>(1)</sup>		Dowel type <sup>(2)</sup>	Gap <sup>(3)</sup> [mm]	No. of tests
				top	bottom			
1	#2, #3	2700	600	B	B	P	0	2
1	#4	2700	300	B	B	P	0	1
1	#5	2700	300	B	B	P	0	1
1	#7	2700	600	B	B	S	0	1
1	#8	2700	300	B	B	S	0	1
1	#9	2700	600	E	B	P	30	1
1	#10, #12	2700	600	E	B	P	20	2
1	#13	2700	600	E	B	S	30	1
1	#14	2700	600	E	B	S	20	1
Total no. of tests								11

<sup>(1)</sup> Horizontal connections between partitions and top and bottom beams (representing the connections between partitions and floors or beams); B: basic connections, E: enhanced anti-earthquake connections.

<sup>(2)</sup> Dowel types; P for Plastic dowel, S for Steel dowels.

<sup>(3)</sup> Gap between sheathing boards and surrounding elements.

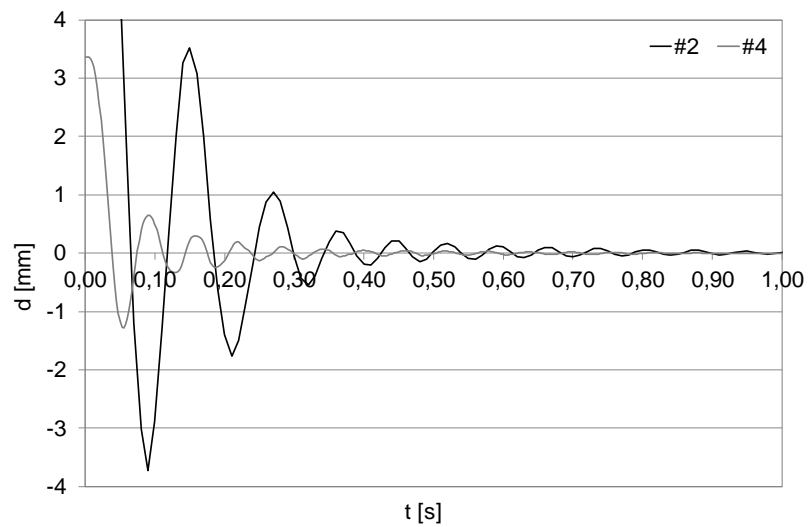


**Fig. 11.** Response curves for out-of-plane dynamic identification tests

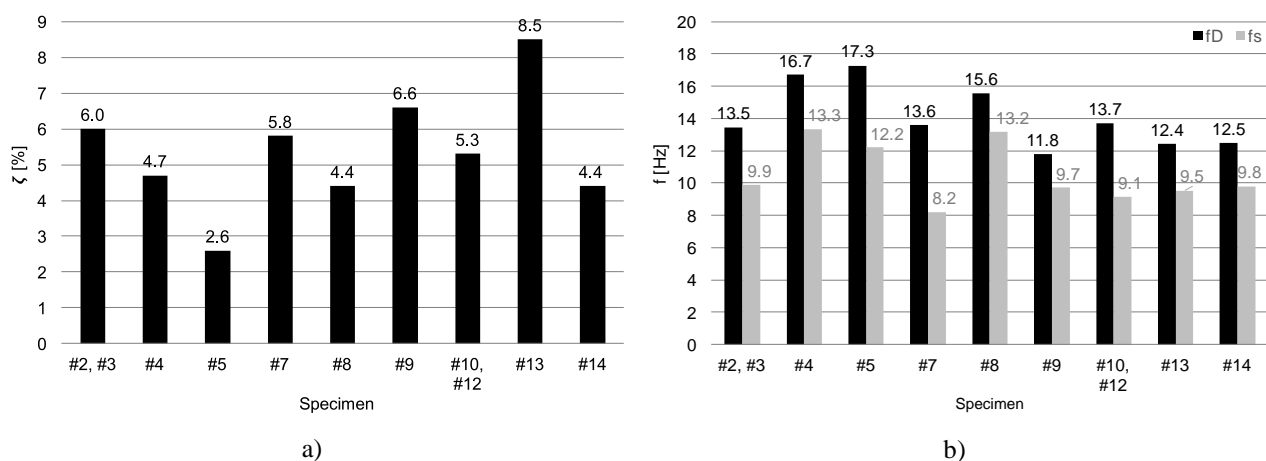


**Fig. 12.** Values of main parameters: a) damping ratio and b) experimental and theoretical fundamental vibration frequencies

The damping ratio was affected primarily by stud spacing (300 or 600 mm), partition-to-surrounding connection types (basic or enhanced anti-earthquake connections) and gap between sheathing boards and surrounding elements (20 or 30 mm for enhanced anti-earthquake connections). As far as the effect of stud spacing is concerned, 300 mm stud spacing partitions, #4, #5 and #8, revealed lower values of damping ratio (from 2.6 to 4.7%) compared to 600 mm stud spacing partitions, #2, #3, #7, #9, #10, #12, #13 and #14 (from 4.4 to 8.5%). Therefore, the results show that the stud spacing produced a reduction of the damping ratio values when spacing ranged from 600 to 300 mm. The partition-to-surrounding connection types influenced also the damping ratio and, in fact, basic-connection partitions, #2, #3 and #7, showed values of damping ratio from 5.8 to 6%, whereas enhanced-connection partitions, #9, #10, #12, #13 and #14, revealed values more scattered (from 4.4 to 8.5%). Therefore, the partition-to-surrounding connection types produced an increasing of the damping ratio values when enhanced-connection were used. Finally, enhanced-connection partitions with a gap equal to 30 mm, #9 and #13, exhibited higher values of damping ratio (from 6.6 to 8.5%) than those obtained for partitions with gap equal to 20 mm, #10, #12 and #14 (from 4.4 to 5.3%).

Test results shows that the partition dynamic response in terms of fundamental vibration frequency was mainly affected by stud spacing (300 or 600 mm) and partition-to-surrounding connection types (basic or enhanced anti-earthquake connections). In fact, 300 mm stud spacing partitions, #4, #5 and #8, exhibited greater values of frequency (from 15.6 to 17.3 Hz) than those obtained for 600 mm stud spacing partitions, #2, #3, #7, #9, #10, #12, #13 and #14 (from 11.8 to 13.7 Hz), by highlighting an increasing of stiffness when the stud spacing ranged from 600 to 300 mm. A similar effect was observed by comparing basic and enhanced anti-earthquake connections, with basic connections (frequency from 13.5 to 17.3 Hz for #2, #3, #4, #5, #7 and #8) stiffer than anti-earthquake connections (frequency from 11.8 to 13.7 Hz for #9, #10, #12, #13 and #14). Therefore, according to the definition of rigid and flexible architectural non-structural components provided by ASCE/SEI 7-10 [1],

partitions with 600 mm stud spacing can be considered as flexible components because they were characterized by values of frequency lower than 16.67 Hz, whereas partitions with 300 mm stud spacing had a borderline behaviour in terms of dynamic stiffness classification. More data about out-of-plane dynamic identification tests are provided in [36].

From the examination of the out-of-plane response, some design implications can be given: (1) partition-to-surrounding connections (basic or enhanced anti-earthquake connections) do not significantly affect the out-of-plane quasi-static response and they can be schematized as simple supports; (2) partition-to-surrounding connections influence the dynamic response, and an increasing of damping ratio and a reduction of fundamental vibration frequency were recorded when enhanced connections were used; (3) the out-of-plane quasi-static response of partitions is affected by stud spacing (300 or 600 mm) and the strength and stiffness doubled their values when 300 mm stud spacing was used; (4) stud spacing influences also the out-of-plane dynamic response of partitions, with a reduction of damping ratio and an increasing of the fundamental vibration frequency for 300 mm stud spacing partitions; (5) a good prevision of the out-of-plane resistance can be obtained by adopting EWM; (6) theoretical estimations of the fundamental vibration frequency give underestimated previsions (26% in average).

#### **4. IN-PLANE TESTS**

In order to experimentally assess the seismic fragility and the related damage levels in accordance with the inter-storey drift ratio (IDR) limits defined by Eurocode 8 Part 1 in Section 4.3.3 for deformation-sensitive components, an experimental campaign involving in-plane quasi-static reversed cyclic tests on partitions (Components 1 and 2) was performed (Fig. 13). In particular, the interaction between partitions and surrounding elements was also taken into account during the research activity. Therefore, 2400 long and 2700 high partitions were used for Components 1 and 2 and 600 long and 2700 high façades were selected as return walls in Components 2.

Different parameters were investigated for defining the experimental program: (1) stud spacing (300 or 600 mm); (2) types of partition-to-surrounding connections (basic or enhanced anti-earthquake connections, as described in Section 2.1 and showed in Fig. 5) for realizing the horizontal and vertical connections between partitions and surrounding elements; (3) sheathing board types (GWB or GFB); (4) jointing finishing types. A total number of 8 and 4 tests were carried out on Components 1 and 2, respectively. Table 4 shows the test matrix.

A specific test set-up was designed to carry out the in-plane cyclic tests (Fig. 14). The test set-up, which replicated the behaviour of a typical storey of a building structure, was a bi-dimensional frame made of S355JR steel grade hot-rolled profiles. The testing frame was made of a bottom beam, a top beam and two hinged columns and it was arranged in two different layouts to perform tests on

Components 1 and 2. Two steel portal frames were used for avoiding the out-of-plane displacements of test set-up. The testing frame was completed with C25/30 strength class 50 mm thick concrete blocks for simulating the interface with a reinforced concrete structure. The tests required a specific instrumentation: (1) 1 linear wire potentiometer used for measuring the top horizontal displacement (i.e, lateral drift); (2) 2 potentiometers adopted for measuring the diagonal displacements of partition; (3) 5 horizontal and 6 vertical LVDTs used for measuring the horizontal and vertical displacements, respectively, between partitions and testing frame (in case of Component 1) or return walls (in case of Component 2).

The in-plane cyclic tests, performed in displacement-controlled test procedure, were carried out by adopting a loading protocol defined according to FEMA 461 [50], which consisted of repeated cycles of step-wise increasing deformation amplitudes. In the specific case, the loading protocol included 18 steps with imposed IDRs, which are defined as the ratios between the recorded displacement (by  $P_1$  in Fig. 14) and the partition height (2700 mm), ranging from 0.08% to 8.40%. The number of steps was selected in order to appreciate the damage of partitions for very small and high IDRs.



**Fig. 13.** In-plane quasi-static reversed cyclic tests: a) test on Component 1; b) test on Component 2

**Table 4.** Test matrix for in-plane quasi-static reversed cyclic tests

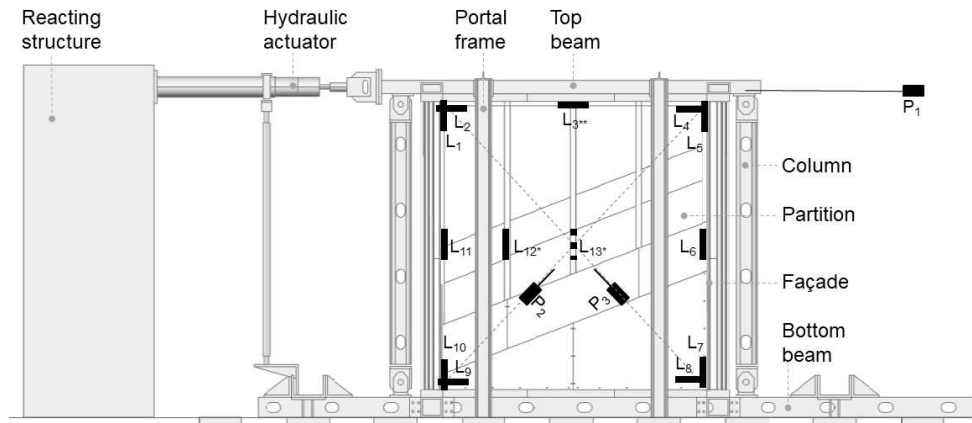
Component	Specimen label	Stud spacing [mm]	Horizontal connections <sup>(1)</sup>		Vertical connections <sup>(2)</sup>	Sheathing board <sup>(3)</sup>	Joint finishing <sup>(4)</sup>		No. of tests
			top	bottom	lateral sides		Field joints	Perimeter joints	
1	#1,	600	B	B	B	GWB	GF	GF	1
1	#2, #3	600	B	B	B	GWB	PT	AT	2
1	#4	300	B	B	B	GWB	PT	AT	1
1	#5	600	B	B	B	GFB	PT	AT	1
1	#6	600	E	B	B	GWB	PT	AT	1
1	#7, #8	600	E	B	E	GWB	PT	AT	2
2	#9, #10	600	B	B	-	GWB	PT	AT	2
2	#11, #12	600	E	B	-	GWB	PT	AT	2
Total no. of tests									12

<sup>(1)</sup> Horizontal connections between partitions and top and bottom beams (representing the connections between partitions and floors or beams): B: basic connections, E: enhanced anti-earthquake connections.

<sup>(2)</sup> Vertical connections between partitions and columns (representing the connections between partitions and columns) in case of Component 1: B: basic connections, E: enhanced anti-earthquake connections.

<sup>(3)</sup> Sheathing boards of partitions; GWB: standard gypsum boards; GFB: gypsum-fibre boards.

<sup>(4)</sup> Partitions joint finishing at the field and perimeter joints (only for basic connections); GF: glass fibre tape with alkaline-resistant coating fixed with gypsum-based plaster; PT: paper tape fixed with gypsum-based plaster; AT: self-adhesive paper tape.



L<sub>i</sub>: linear variable differential transducers  
P<sub>i</sub>: linear wire potentiometers

\*: transducer used for the tests on specimens #2, #3, #4 and #5

\*\* : transducer used for the tests on specimens #6, #7 and #8

**Fig. 14.** Test set-up and adopted instrumentation

Response curves were provided in terms of load (F) versus IDR. For the sake of brevity, Fig. 15 shows only the response curves obtained for #1 and #12 specimens (Component 1). The hysteretic behaviour of partitions was strongly characterized by pinching phenomenon, stiffness and strength degradation when IDR increased. Fig. 16 plots the first cycle envelope curves of the hysteretic responses for Components 1 and 2. The obtained first cycle envelope curves show that partitions with basic-connection, #1, #2, #3, #4, #5, #9 and #10, provided additional strength and stiffness to the surrounding elements starting from the initial phase of the response. On the contrary, partitions with

enhanced-connection, #6, #7, #8, #11 and #12, provided additional strength and stiffness for more high IDRs, i.e. when the contact between sheathing boards and surrounding elements was restored.

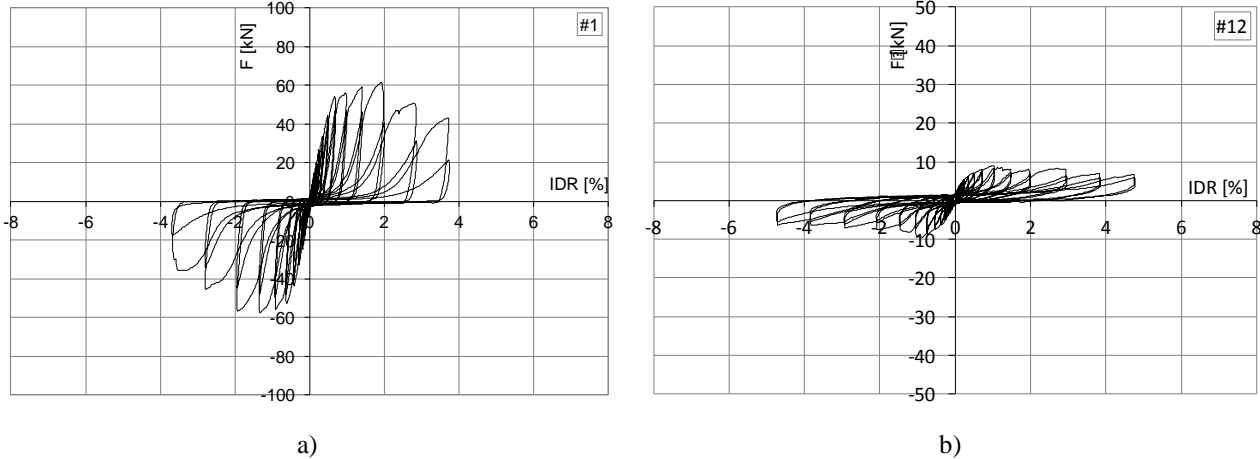


**Fig. 15.** Response curves for in-plane quasi-static reversed cyclic tests on Component 1: (a) #1 specimen; (b) #2 specimen

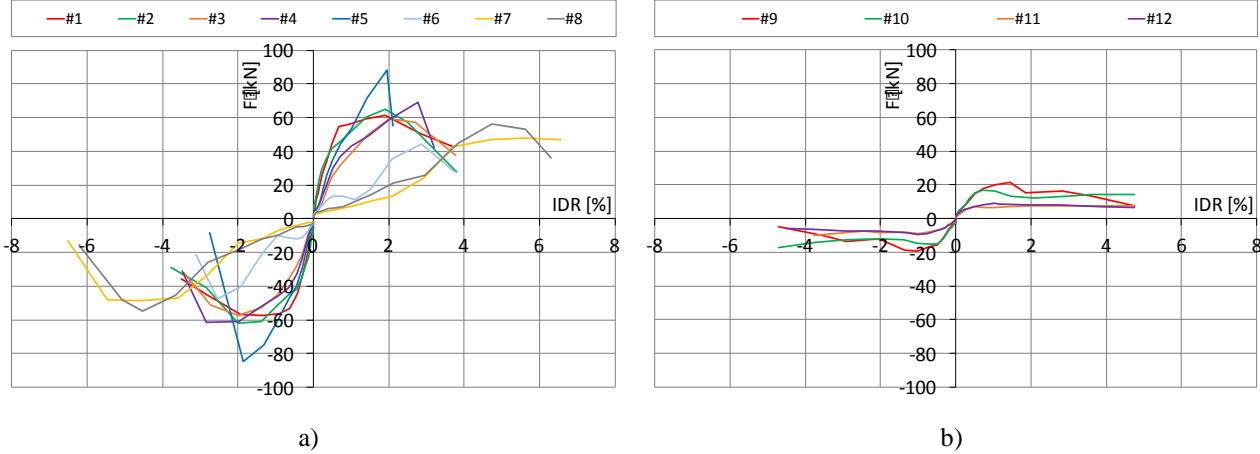


**Fig. 16.** First cycle envelope curves for: (a) Component 1; (b) Component 2

The parameters used to describe the experimental behaviour were the recorded maximum and minimum strengths ( $F$ ) and the secant stiffness ( $k_s$ ) evaluated for the maximum and minimum loads reached during the tests. Test results and the average values for configurations with more nominally identical specimens are presented in Fig. 17 for Components 1 and 2 in terms of secant stiffness and strength.

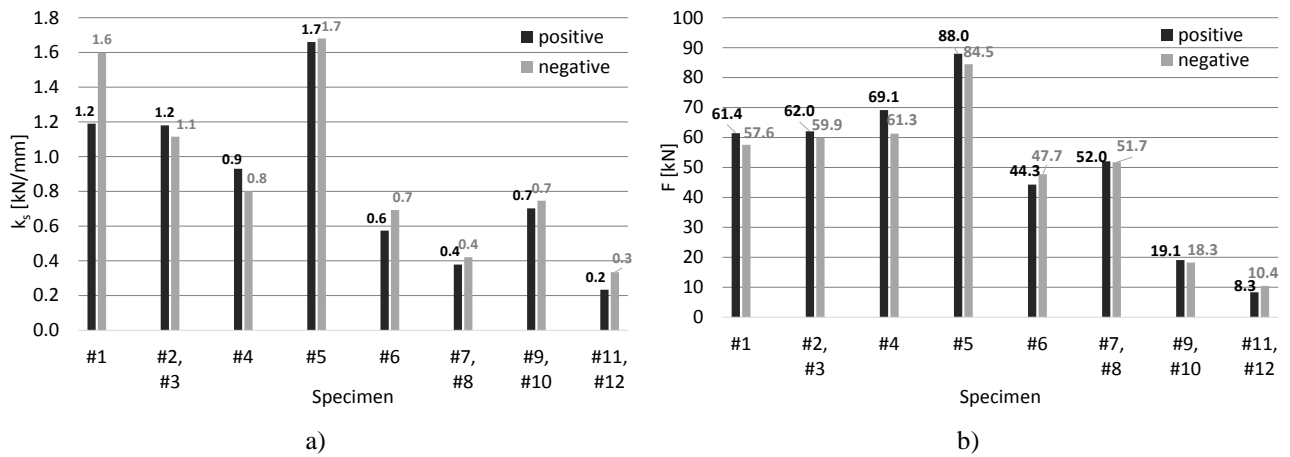


**Fig. 17.** Values of main parameters: a) secant stiffness and b) strength

The results show that the experimental response was strongly affected by the partition-to-surrounding connection types (basic or enhanced anti-earthquake connections) and sheathing board types (GWB or GFB). In fact, as far as Component 1 is concerned, basic-connection partitions, #1 through #5, revealed higher values of secant stiffness (from 0.8 to 1.7 kN/mm) and strength (from 57 to 88 kN) than enhanced-connection partitions, #6 through #8 (from 0.4 to 0.7 kN/mm for stiffness and from 44 to 52 kN for strength). Also in case of Component 2, basic-connection partitions, #9 and #10, revealed higher values of secant stiffness (about 0.7 kN/mm) and strength (from 18.3 to 19.1 kN) than enhanced-connection partitions, #11 and #12 (from 0.2 to 0.3 kN/mm for stiffness and from 8 to 10 kN for strength). Finally, the adoption of GFBs, #5, involved higher secant stiffness (1.7 kN/mm) and strength (from 85 to 88 kN) respect to the values recorded for GWBs, #1 through #4 (from 0.8 to 1.2 kN/mm for stiffness and from 58 to 69 kN for strength). The effects of stud spacing and joint finishing types played a secondary role on the experimental behaviour in terms of stiffness and strength. Furthermore, the difference between the values of secant stiffness and strength recorded in the positive and negative directions was not significant (with maximum difference within 13%), except for the secant stiffness recorded for specimen #1 (negative stiffness about 1.3 higher than positive stiffness). However, the higher difference in terms of secant stiffness recorded for the specimen #1 could be due to jointing finishing at the field and perimeter joints realized with glass fibre tape with alkaline-resistant coating fixed with gypsum-based plaster, which was characterized by a behaviour more brittle than that observed for joints realized with paper tape fixed with gypsum-based plaster for field joints and self-adhesive paper tape for perimeter joints (specimens #2 and #3). As a result of a brittle behaviour of jointing finishing, the strength degradation for negative cycles occurred before than that observed for positive cycles, with a resulting peak strength occurred for a displacement less than that observed for positive cycles. The evaluation of seismic fragility of the tested components is provided in Section 6. More data concerning the in-plane cyclic tests are given in [34].

## 5. SHAKE TABLE TESTS

Shake table tests were performed for evaluating experimentally the dynamic properties, dynamic amplification and seismic fragilities of partitions, façades and ceilings. Tests were carried out by means of the shaking-table available at the Department of Structures for Engineering and Architecture at the University of Naples “Federico II” having plan dimensions of 3.0×3.0 m, two horizontal degrees of freedom, maximum payload of 200 kN, frequency range of 0-50 Hz, peak acceleration of 1.0 g (for the maximum pay load), peak velocity of 1.0 m/s and displacement in the range of ±250 mm.

The test set-up (Fig. 18), representative of a reinforced concrete bare structure was made of a bottom and a top steel beam grid connected by four columns. The lateral structural restraint systems in the shaking direction (E-W direction) was an eccentric bracing system, in which diagonal members were pretensioned truss elements with rectangular cross section, whereas in N-S direction the test set-up was braced by means of X-bracings made of steel cables. A concrete block with a weight of 340 kN was placed on the top beam grid for obtaining the desired system mass. All frame members were fabricated with S355JR steel grade, whereas the diagonal truss members were made of ultra-high strength steel (steel grade REAX 450 with yielding and ultimate strength equal to 1250 and 1450 MPa, respectively). Also in this case, the testing frame was completed with C25/30 strength class 50 mm thick concrete blocks for simulating the interface with a reinforced concrete structure.



**Fig. 18.** Test set-up

Shake table tests were carried out on two assemblages of different components (Fig. 19): (1) Assembly 1 composed by four partitions (Components 1) placed in both E-W and N-S directions; (2) Assembly 2 consisting of two partitions (Components 2) placed in N-S direction, two façades (Components 3) placed in E-W direction and one ceiling (Component 4). In particular, the partitions placed in the shaking direction (E-W direction) in Assembly 1 had dimensions equal to 2400×2700

mm (length × height), the façades placed in the shaking direction (E-W direction) in Assembly 2 had dimensions equal to 2400×2700 mm (length × height) and the ceiling adopted in Assembly 2 had dimensions equal to 1675×2300 mm (length in E-W direction × length in N-S direction). For both Assemblages 1 and 2, the solutions with basic and enhanced anti-earthquake connections were investigated. A total number of 3 and 2 prototypes were tested on Assemblages 1 and 2, respectively. Table 5 shows the test matrix.



**Fig. 19.** Shake table tests: a) tests on Assembly 1; b) tests on Assembly 2

**Table 5.** Test matrix for shake table tests

Assembly	Prototype label	Component			Horizontal connections <sup>(1)</sup>		Vertical connections <sup>(2)</sup>	No. of tests
		E-W direction	N-S direction	-	top	bottom	lateral sides	
1	#1, #2	1	1	-	B	B	B	2
1	#3	1	1	-	E	B	E	1
2	#4	3	2	4	B	B	B	1
2	#5	3	2	4	E	B	E	1
Total no. of tests								5

<sup>(1)</sup> Horizontal connections between partitions (or façades) and top and bottom beams (representing the connections between partitions or façades and floors or beams): B: basic connections (as described in Section 2.1 and showed in Fig. 5), E: enhanced anti-earthquake connections (as described in Section 2.1 and showed in Fig. 5).

<sup>(2)</sup> Vertical connections between partitions (or façades) and columns (representing the connections between partitions or façades and columns): B: basic connections (as described in Section 2.1 and showed in Fig. 5), E: enhanced anti-earthquake connections (as described in Section 2.1 and showed in Fig. 5).

As far as the instrumentation is concerned, 12 triaxial accelerometers and 9 laser sensors, arranged with three different layouts for the tests on the bare structure (i.e. test setup) and Assemblages 1 and 2, were adopted. In particular, laser sensors were placed on the bare structure, partitions and façades for measuring displacements, whereas accelerometers were placed on the top mass, partitions, façades and ceilings for measuring accelerations.

The seismic input was a unidirectional acceleration time history artificially defined to match the Required Response Spectrum (RRS) provided by ICBO-AC156 code [51] acting along the E-W direction. The RRS was selected for a ground motion with a design spectral acceleration at short

period ( $S_{DS}$ ) equal to 1.0g, corresponding to a peak ground acceleration ( $a_g$ ) equal to 0.4g, representative of an earthquake having 10% probability of exceedance in 50 years in a high seismicity zone (Fig. 20). According to ICBO-AC156 code, the acceleration spectrum of the selected acceleration time history shall be in the range from 90% to 130% of RRS and the matching procedure shall be valid for a frequency range from 1.3 to 33.3 Hz. The selected input time history was applied with different scaling factors (SFs) in the range from 5% to 120%, corresponding to a maximum horizontal flexible acceleration ( $A_{FLEX,H}$  in ICBO-AC156, which represents the maximum spectral acceleration) ranging from 0.08 g to 1.92 g, i.e. SF=100% corresponds to  $a_g=0.4g$ ,  $S_{DS}=1.0g$ , and  $A_{FLEX,H}=1.6g$ . Dynamic identification tests were carried out before and after each input by applying a white noise signal.

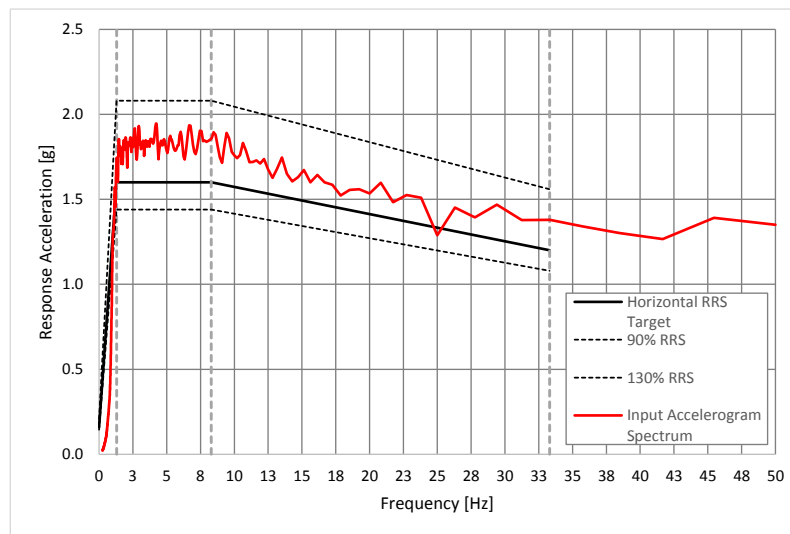


**Fig. 20.** Input spectrum vs. RRS target for SF=100% (corresponding to  $a_g=0.4g$ ,  $S_{DS}=1.0g$ ,  $A_{FLEX,H}=1.6g$ )

The dynamic identification tests were interpreted for evaluating the fundamental vibration frequency and damping ratio of the bare structure and Assemblages 1 and 2. In particular, the fundamental frequencies were calculated as the first peak of the frequency response function (or transfer function) in the frequency domain. The frequency response functions (magnitude vs. frequency curves) were obtained as the ratio between the Fourier transformation of the input signal and the response signals corresponding to the data of accelerometers installed on the top mass. Fig. 21 plots fundamental frequency ( $f$ ) versus scaling factors (SF). Results show that the non-structural components provided an increment of the fundamental vibration frequency of the bare structure (2.9 Hz) up to 10.3 and 14.0 Hz in case of Assembly 1 (partitions) and Assembly 2 (partitions, façades and ceiling), respectively. Generally, the fundamental vibration frequency of Assemblages 1 and 2 decreased as input intensity increased due to the increment of damage levels achieved in the non-structural components during the tests. At the end of the tests, the fundamental vibration frequency of the Assemblages 1 and 2 was almost equal to that of the bare structure. In addition, the Assemblages 1

and 2 with enhanced-connections reached higher values of fundamental vibration frequency (up to 10.2 Hz for #3 and 14 Hz for #5) than the Assemblages 1 and 2 with basic-connections (up to 7.2 Hz for #1, 10.3 Hz for #2, and 13.2 Hz for #4). It should be noted that, in the case of assemblages of the same typologies, #1 e #2, the values of fundamental frequency are strongly different because the adopted loading histories are several and, therefore, the evolution of damages is different between the two assemblages.

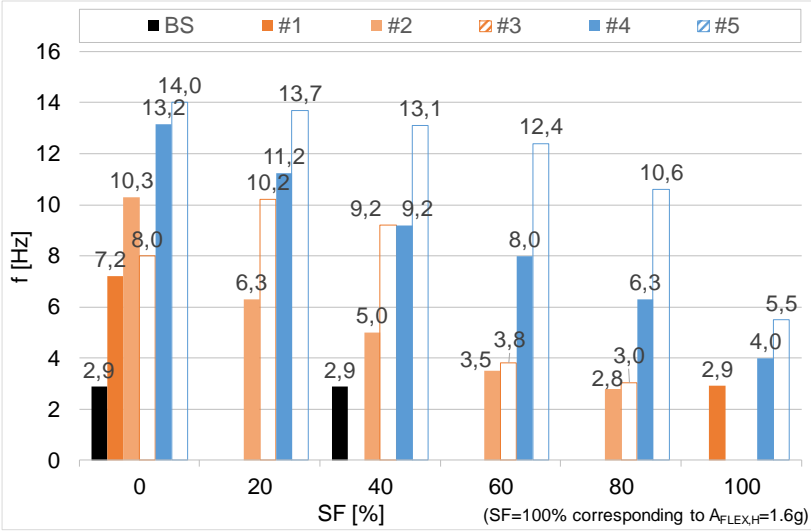


**Fig. 21.** Fundamental frequency versus scaling factors

The presence of non-structural components also increased the damping ratio of the bare structure (ranging from 4.0% to 4.8%). Fig. 22 shows damping ratio ( $\zeta$ ) versus scaling factors (SF). The results reveal that, in a first phase, the damping ratio increased as the input intensity increased, whereas, in a second phase, it decreased due to the significant level of damage of non-structural components (except for the prototype #5). The type of partition or façade-to-surrounding connections influenced the damping ratio and, in fact, Assembly 1 and 2 with enhanced anti-earthquake connections reached higher values of damping ratio (up to 20% for #3 and #5) respect to the values recorded for Assembly 1 and 2 with basic connections (up to 13% for #1, #2 and #4). It should be noticed that the recorded damping takes into account all phenomena, e.g. the component cracking. Other studies demonstrated that the change in terms of damping ratio during the different seismic tests is correlated to the recorded damages. In particular, for specimens similar to the Assembly 1 with basic connections damping ratio values ranging between 9.3% and 17.3% (with the maximum recorded for a drift level corresponding to the maximum shear strength) were recorded by McCormick et al. [37] and a value of 8% was found in Magliulo et al. [39].

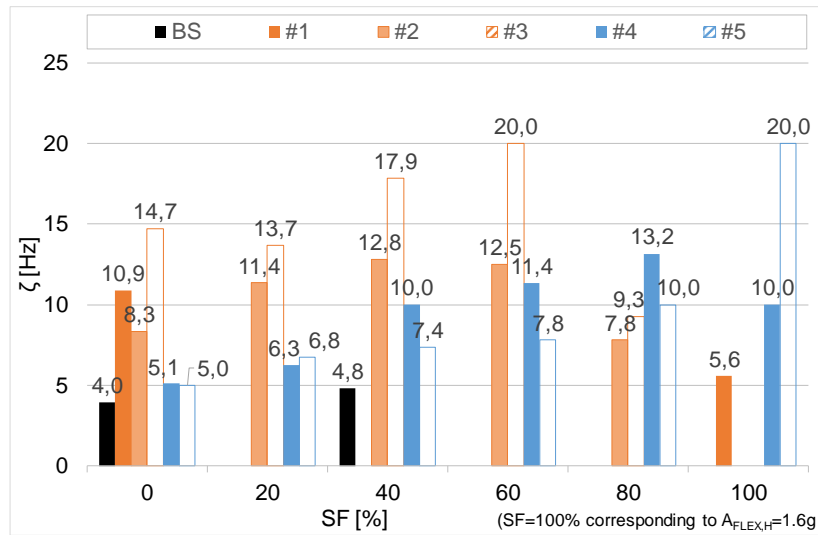


**Fig. 22.** Damping ratio versus scaling factors

The non-structural components affect significantly the structural lateral response. This observation is revealed by Fig. 23 that plots the floor acceleration (FA) versus IDR curves for prototypes #1 and #3, where FA is the average value of the accelerations recorded at the top mass. Assembly 1 and 2 with basic connections, #1, #2 and #5, strongly influenced the initial lateral response by providing additional strength and stiffness to the bare structure. On the contrary, Assembly 1 and 2 with enhanced anti-earthquake connections, #3 and #5, did not affect the initial response until the contact between sheathing boards and surrounding elements was restored, by observing a strengthening effect for drifts larger than about 2%.

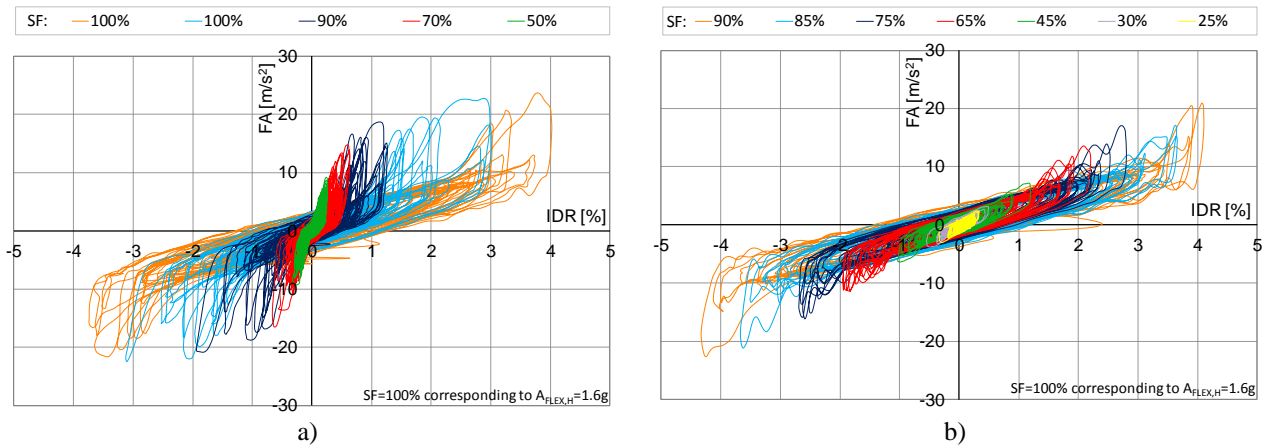


**Fig. 23.** FA versus IDR curves for selected SF (%) of ICBO-AC156 input for Assembly 1: a) Prototype #1; b) Prototype #3

The dynamic amplification of tested components can be evaluated by comparing the peak component acceleration (PCA) and the peak bare structure acceleration (PBA) measured by accelerometers installed on components and bare structure, respectively. In particular, the unidirectional tests were representative of: a) in-plane response of Components 1 and Components 3; b) out-of-plane response of Components 1 and Components 2 and c) in-plane response of Components 4. Fig. 24 shows the

curves related to the in-plane dynamic amplification for Components 1 and 3 and Fig. 25 shows the curves relevant to the out-of-plane dynamic amplification for Components 1 and 2. In particular, Figures plot PCA vs. PBA, together with the lines representing different values of PCA-to-PBA ratio, which represents the acceleration amplification factor ( $\alpha_c$ ). The examination of test results points out that the dynamic amplification increased as PBA increased, due to the reduction of stiffness caused by the increment of damages of components. The acceleration amplification for in-plane response was in the range from 1 to 4 for Component 1 (partitions), #1, #2 and #3, and from 1 to 3 for Component 3 (façades), #4 and #5. Regarding the effect of the partition or façade-to-surrounding connection types, Assembly 1 and 2 with enhanced anti-earthquake connections (#3 and #5) revealed a more flexible behaviour with higher values of the in-plane acceleration amplification (up to 4 and to 3 for Component 1 – partitions - and Component 3 – façades -, respectively) respect to Assemblages 1 and 2 with basic connections (#1, #2 and #4) with values up to 2 for both Component 1 (partitions) and Component 3 (façades). Furthermore, the acceleration amplification for out-of-plane response of Component 1 and 2 (partitions), #1, #2, #3, #4 and #5, and in-plane response of Component 4 (ceiling) were in the range from 1 to 2. The evaluation of the seismic fragility of the tested components is provided in Section 6. The performed shake table tests are discussed in detailed manner in [45].

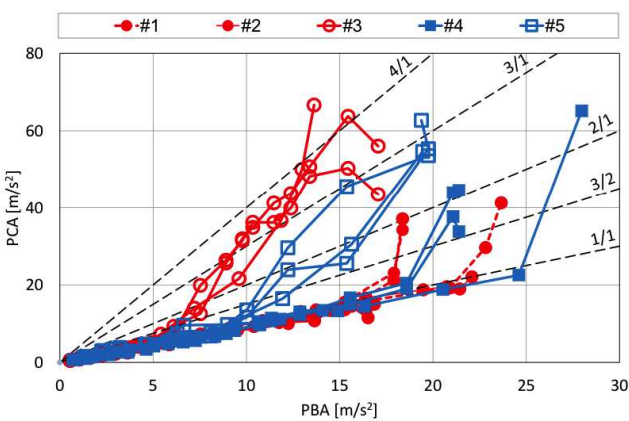


**Fig. 24.** In-plane dynamic amplification for Components 1 and 3

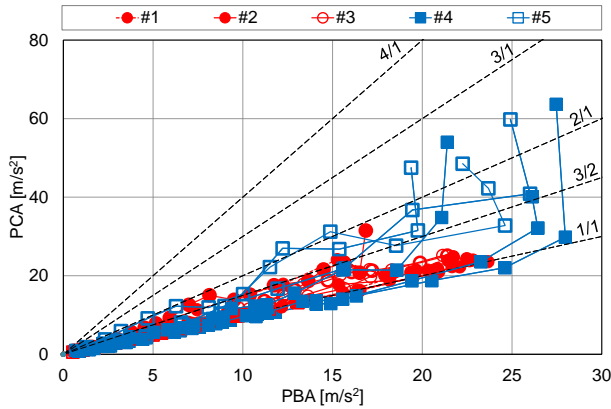


**Fig. 25.** Out-of-plane dynamic amplification for Components 1 and 2

**6. SEISMIC FRAGILITY EVALUATION FOR IN-PLANE RESPONSE**

The seismic fragility evaluation was performed by elaborating test results obtained by both in-plane quasi-static reversed cyclic tests and shake table tests. In particular, the proposed fragility curves refer to the in-plane seismic response of Components 1, 2 and 3. A procedure articulated in 5 steps was adopted for developing fragility curves.

Firstly (step 1), three damage limit states (DSs) were evaluated on the base of a large database of tests. In particular, eight quasi-static racking tests on gypsum sheathed LWS partitions used in the most spread buildings [25], in-plane quasi-static and dynamic tests conducted on thirty-six gypsum

sheathed LWS partitions constructed using common construction details [30], six quasi-static tests performed on 5-m-high gypsum sheathed LWS partitions commercialized in Europe for industrial buildings [31] were considered for classifying the DSs. The DSs were defined according to the observed damage level and the required repair action as following: DS1, which is characterized by superficial damage and it requires minimum repair with plaster, tape and paint; DS2, which is characterized by local damage of sheathing boards and/or steel frame and it requires the replacement of few elements (boards and/or local repair of steel profiles); DS3, which is characterized by severe damage and it requires the replacement of significant parts or whole non-structural component.

Then (step 2), the damage phenomena were observed during the experimentation by means of visual inspection and classified as following: (1) drop of gypsum and/or plaster dust; (2) detachment of joint tape; (3) crack in joints; (4) detachment between walls and surrounding structural elements; (5) crack in panels; (6) corner crushing of panels; (7) local plastic deformations of studs; (8) rupture of panel portions; (9) collapse of board-to-frame fixings, due to screw tilting and pull-out from frame or pull-through in panel and/or breaking of panel edge; (10) collapse of dowels, due to pull-out from surrounding elements; (11) detachment between partitions and façades; (12) out-of-plane collapse of panels; (13) wall out-of-plane collapse. The damage phenomena from (1) to (4) were observed in the initial phase of tests, phenomena from (5) to (10) occurred in the intermediate phase, whereas phenomena from (11) to (13) were detected in the final phase. Fig. 26 shows some damage phenomena for Components 1, 2 and 3 observed during the in-plane cyclic tests and shake table tests. In particular, as far as the shake table tests are concerned, the damages were observed only in Components 1 and 3 placed in the shaking direction (E-W direction). Limited damages were detected for Components 2 located in N-S direction and Components 4.

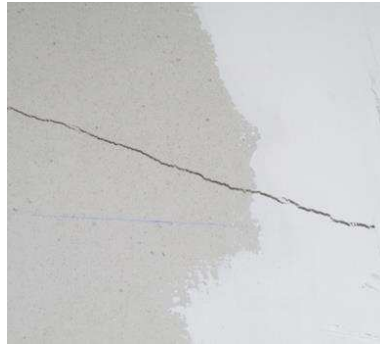
Subsequently (step 3), the damage phenomena were correlated to the DSs. Table 6 shows damage phenomena that triggered the respective DSs and distinguishes the cases of in-plane cyclic and shake table tests. In some cases, like the detachment between partitions or façades and surrounding elements, rupture of board portions, collapse of board-to-frame fixings and collapse of dowels, the triggered DSs depended by the level of the produced damage.

Therefore (step 4), because the in-plane behaviour is primarily governed by IDRs, the damage phenomena were associated to the IDR levels at which each phenomenon started. Table 7 and Table 8 show the minimum values of IDRs for which a defined DS is triggered for each prototype subjected to in-plane tests and shake table tests.

Finally (step 5), the seismic fragility assessment of the tested components was performed by elaborating test results for developing fragility curves. Fragility curves were evaluated according to the method 'A' indicated by Porter et al. [52].



4. detachment between partitions or façades and surrounding elements



5. crack in boards



6. corner crushing of boards



7. local plastic deformations of studs



8. rupture of board portions



9. collapse of board-to-frame fixings



10. collapse of dowels



11. detachment between partitions and façades



12. out-of-plane collapse of boards



13. Out-of-plane collapse of partitions or façades

**Fig. 26.** Observed damage phenomena in in-plane cyclic and shake table tests

**Table 6.** Correlation between observed damage phenomena and damage limit states (DSs)

Observed damage phenomena	DS1 <sup>(1)</sup>		DS2 <sup>(1)</sup>		DS3 <sup>(1)</sup>	
	QS <sup>(2)</sup>	D <sup>(2)</sup>	QS <sup>(2)</sup>	D <sup>(2)</sup>	QS <sup>(2)</sup>	D <sup>(2)</sup>
1. Drop of gypsum and/or plaster dust <sup>(i)</sup>	•	•				
2. Detachment of joint tape <sup>(i)</sup>	•	•				
3. Crack in joints <sup>(ii)</sup>	•					
4. Detachment between partitions or façades and surrounding elements <sup>(i)</sup> , (a)	•		•	•		
5. Crack in boards <sup>(i)</sup>			•	•		
6. Corner crushing of boards <sup>(i)</sup>			•	•		
7. Local plastic deformations of studs <sup>(ii)</sup>			•			
8. Rupture of board portions <sup>(i), (b)</sup>			•		•	•
9. Collapse of board-to-frame fixings <sup>(i), (c)</sup>			•	•	•	
10. Collapse of dowels <sup>(ii), (d)</sup>			•		•	
11. Detachment between partitions and façades <sup>(ii)</sup>					•	
12. Out-of-plane collapse of boards <sup>(i)</sup>					•	•
13. Out-of-plane collapse of partitions or façades <sup>(ii)</sup>					•	

<sup>(i)</sup> Damage phenomena observed in both in-plane cyclic and shake table tests.  
<sup>(ii)</sup> Damage phenomena observed only in in-plane cyclic tests.  
<sup>(1)</sup> Damage limit states.  
<sup>(2)</sup> Test typology; QS: in-plane quasi-static reversed cyclic tests, D: dynamic shake table tests.  
<sup>(a)</sup> Maximum detachment  $\leq 5$  mm for DS1 and  $> 5$  mm for DS2; <sup>(b)</sup> Involved board surface  $\leq 50$  cm<sup>2</sup> for DS2 and  $> 50$  cm<sup>2</sup> for DS3; <sup>(c)</sup> Involved board-to-frame fixings  $\leq 5$  % for DS2 and  $> 5$  % for DS3; <sup>(d)</sup> Involved dowels  $\leq 5$  % for DS2 and  $> 5$  % for DS3

**Table 7.** Minimum IDR levels for which the DSs were triggered in case of Component 1

Component	1										
	B <sup>(1)</sup>					E <sup>(1)</sup>					
Partition or façade-to- surrounding connections	B <sup>(1)</sup>					E <sup>(1)</sup>					
Test typology	QS <sup>(2)</sup>					D <sup>(2)</sup>		QS <sup>(2)</sup>			D <sup>(2)</sup>
Prototypes/minimum IDRs [%]	#1	#2	#3	#4	#5	#1* E / W <sup>(3)</sup>	#2* E / W <sup>(3)</sup>	#6	#7	#8	#3* E / W <sup>(5)</sup>
DS1	0.35	0.22	0.28	0.65	0.51	0.32/0.32	0.28/0.40	1.1	1.3	1.3	0.89/0.89
DS2	1.34	0.96	0.97	1.02	1.02	0.66/0.66	1.19/1.19	1.5	1.5	1.5	1.39/2.21
DS3	1.91	1.40	1.43	1.45	1.32	3.12/3.12	3.20/3.20	2.0	2.1	2.1	> 4.33

<sup>(1)</sup> Partition or façade-to-surrounding connections; B: basic connections, E: enhanced anti-earthquake connections.

<sup>(2)</sup> Test typology; QS: in-plane quasi-static reversed cyclic tests, D: dynamic shake table tests.

<sup>(3)</sup> E: Partition/façade that filled up the east side, W: Partition/façade that filled up the west side (See Fig. 19).

**Table 8.** Minimum IDR levels for which the DSs were triggered in cases of Components 2 and 3

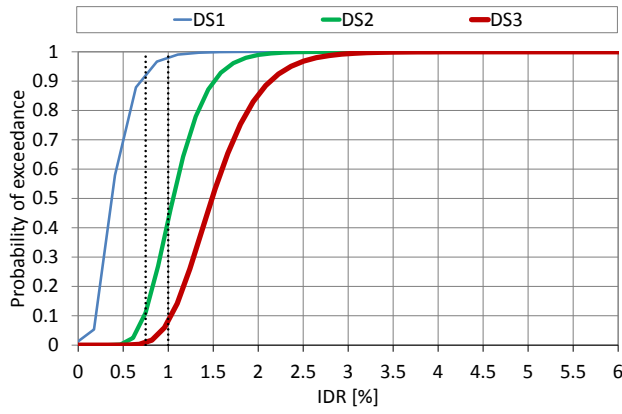
Component	2				3	
Partition or façade-to- surrounding connections	B <sup>(1)</sup>		E <sup>(1)</sup>		B <sup>(1)</sup>	E <sup>(1)</sup>
Test typology	QS <sup>(2)</sup>				D <sup>(2)</sup>	
Prototypes/minimum IDRs [%]	#9	#10	#11	#12	#4* E / W <sup>(3)</sup>	#5* E / W <sup>(3)</sup>
<b>DS1</b>	0.51	0.72	0.47	0.50	1.11/1.11	1.11/1.11
<b>DS2</b>	1.35	1.42	1.02	1.01	2.44/3.23	2.44/3.23
<b>DS3</b>	2.04	2.10	1.42	1.47	4.54/4.54	4.54/4.54

<sup>(1)</sup> Partition or façade-to-surrounding connections; B: basic connections, E: enhanced anti-earthquake connections.

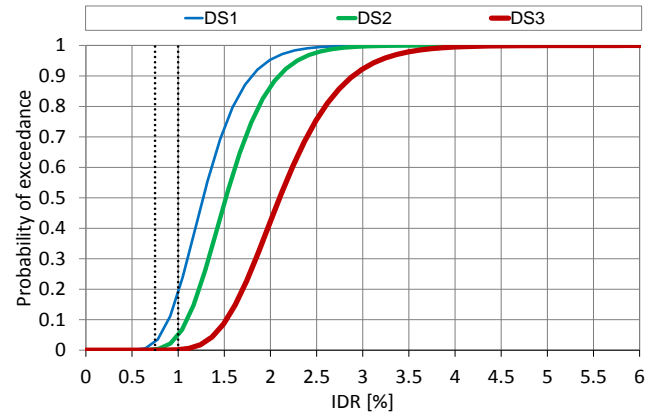
<sup>(2)</sup> Test typology; QS: in-plane quasi-static reversed cyclic tests, D: dynamic shake table tests.

<sup>(3)</sup> E: Partition/façade that filled up the east side, W: Partition/façade that filled up the west side (See Fig. 19).

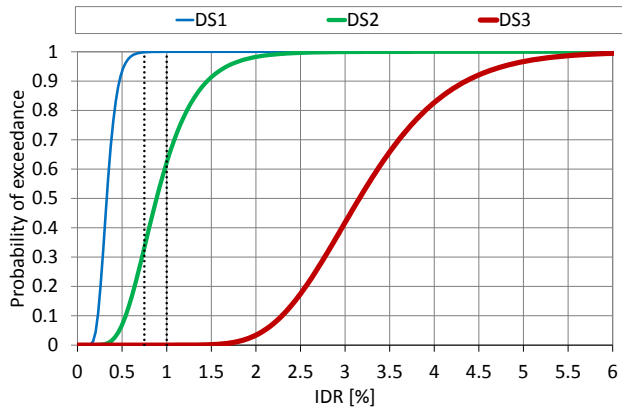
The obtained fragility curves can be considered acceptable because they satisfy the Lilliefors goodness-of-fit test at the 5% significance level [53]. In this context, it is crucial to note that a fragility curve expresses the damage probability of a given components due to the uncertainty in the system and it should be obtained considering the results of tests carried out on many nominally identical prototypes. However, because the behaviour of tested components was particularly affected by component typology (Components 1, 2 and 3), partition or façade-to-surrounding connections (basic vs. enhanced anti-earthquake connections) and loading protocol (quasi-static cyclic vs dynamic shake table), all other variations were neglected and the fragility data were collected in eight Groups: (A) Components 1 with basic connections subjected to quasi-static loading; (B) Components 1 with enhanced connections subjected to quasi-static loading; (C) Components 1 with basic connections subjected to dynamic loading; (D) Components 1 with enhanced connections subjected to dynamic loading; (E) Components 2 with basic connections subjected to quasi-static loading; (F) Components 2 with enhanced connections subjected to quasi-static loading; (G) Components 3 with basic connections subjected to dynamic loading; (H) Components 3 with enhanced connections subjected to dynamic loading. Fig. 27 shows the fragility functions for the selected Groups, together with the IDR limits given by Eurocode 8 Part 1 (dotted vertical lines), i.e. 0.75% for buildings having ductile non-structural components and 1.00% for buildings having ductile non-structural components fixed in a way so as not to interfere structural deformations.



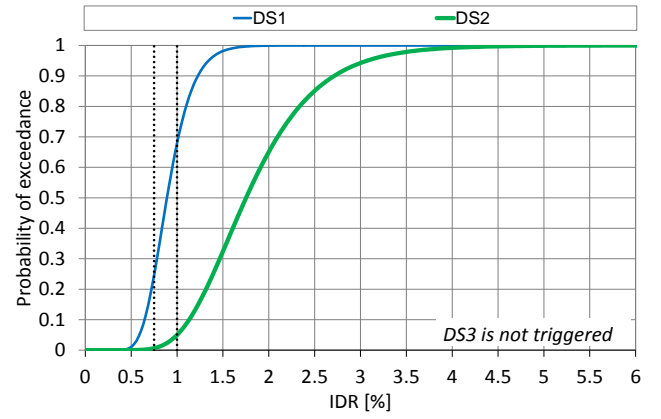
A. Components 1 with basic connections subjected to quasi-static loading



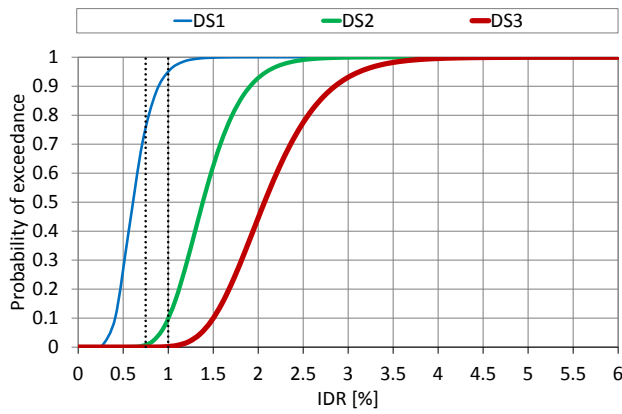
B. Components 1 with enhanced connections subjected to quasi-static loading



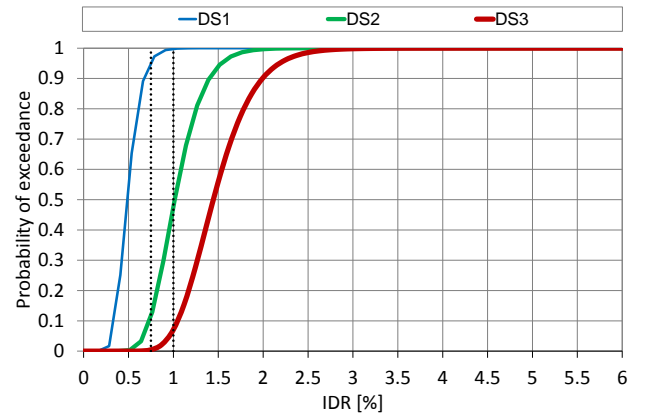
C. Components 1 with basic connections subjected to dynamic loading



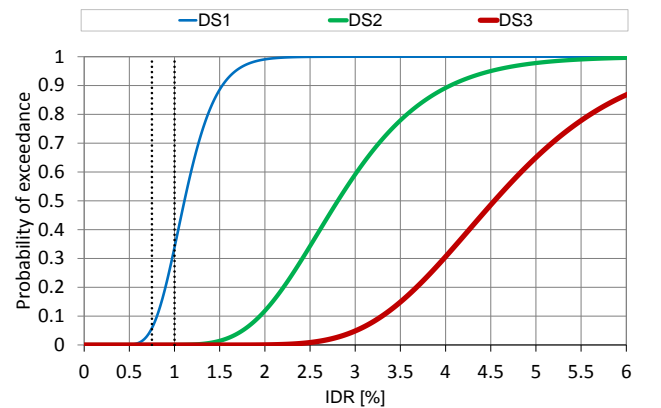
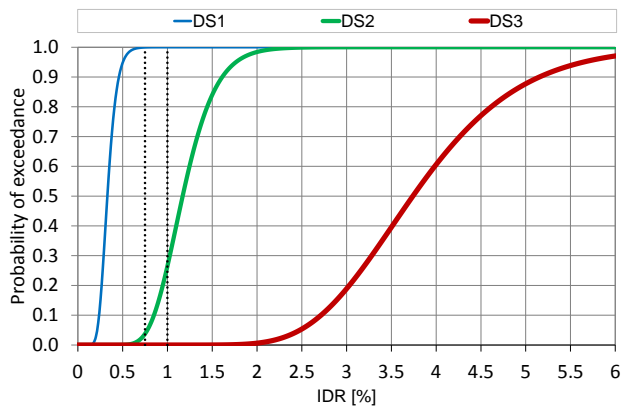
D. Components 1 with enhanced connections subjected to dynamic loading



E. Components 2 with basic connections subjected to quasi-static loading



F. Components 2 with enhanced connections subjected to quasi-static loading



G. Components 3 with basic connections subjected to dynamic loading

H. Components 3 with enhanced connections subjected to dynamic loading

**Fig. 27.** Fragility curves

Table 9 provides the values of fragility parameters in terms of median value ( $x_m$ ) and standard deviation ( $\beta$ ) of the lognormal distribution obtained for each selected Group and DSs. The seismic fragility of the tested components was affected by the partition or façade-to-surrounding connections types (basic or enhanced anti-earthquake connections) and loading protocol (quasi-static or dynamic). Regarding the effect of the partition or façade-to-surrounding connection types, the results for Components 1 and 3 confirm that the adoption of enhanced anti-earthquake connections was more advantageous than basic connections (A vs. B, C vs. D, G vs. H) in terms of reduction of seismic vulnerabilities. In fact, in both Components 1 and 3 with enhanced anti-earthquake connections, the DSs were triggered for median values from 1.2 to 3.4 times greater than the ones recorded for Components 1 and 3 with basic connections. On the other hand, the results for Components 2 show that basic connections had a better behaviour than enhanced anti-earthquake connections (E vs. F), with median values obtained for basic connections from 1.1 to 1.2 times higher than the ones recorded for enhanced anti-earthquake connections. The inefficacy of enhanced anti-earthquake connections in case of Components 2 was due to the inability of return walls to accommodate the lateral in-plane displacements imposed by the transversal partitions.

As far as the influence of the loading protocol is concerned, the comparison between Components 1 subjected to quasi-static loading and dynamic loading (A vs. C and B vs. D) underlines that, for both basic and enhanced anti-earthquake connections, components subjected to dynamic loading revealed median values lower than the ones recorded under quasi-static loading for DS1, whereas components subjected to dynamic loading showed median values higher than the ones recorded under quasi-static loading for DS3. For DS2 an opposite result was found for basic and enhanced anti-earthquake connections, i.e. components with basic connections subjected to dynamic loading revealed median values lower than the ones recorded under quasi-static loading, whereas components with enhanced anti-earthquake connections subjected to dynamic loading revealed median values higher than the ones recorded under quasi-static loading.

Finally, the comparison between partitions and facades can be carried out by comparing the behaviour of Components 1 and Components 3 subjected to shake table loading (C vs G for basic connections and D vs H for enhanced anti-earthquake connections). The results show that façades had a lower seismic vulnerability than partitions. In fact, for components with both basic and enhanced anti-earthquake connections façades triggered the DSs for median values greater than the ones recorded for partitions, excepted for components with enhanced anti-earthquake connections in case of DS3.

Furthermore, Table 9 shows for each Group the probabilities of exceeding the defined DSs considering the IDR limits given by Eurocode 8 Part 1, i.e. 0.75% and 1.00%. Considering a reasonable limit for the probability of exceedance equal to 5%, and assuming the most onerous results between quasi-static cyclic and shake table test results, it is possible to group the components in three different fragility Classes: (1) components with high fragility, i.e. Groups A/C, and F (Components 1 with basic connections and Components 2 with enhanced anti-earthquake connections), for which an IDR of 0.75% can be considered an adequate limit for DS3; (2) components with intermediate fragility, i.e. Groups B/D, E and G (Components 1 with enhanced anti-earthquake connections, Components 2 and Components 3 with basic connections), for which IDRs of 0.75% and 1.00% can be considered adequate limits for DS2 and DS3, respectively; (3) components with low fragility, i.e. Group H (Components 3 with enhanced anti-earthquake connections), for which an IDR of 1.00% can be considered an adequate limit for DS2.

**Table 9.** Fragility parameters

Component group	Description	DS1		DS2		DS3	
		$x_m$ [%]	$\beta$ [-]	$x_m$ [%]	$\beta$ [-]	$x_m$ [%]	$\beta$ [-]
A	Components 1 with basic connections subjected to quasi-static loading	0.37	0.51	1.05	0.29	1.49	0.29
B	Components 1 with enhanced connections subjected to quasi-static loading	1.27	0.28	1.52	0.25	2.10	0.25
C	Components 1 with basic connections subjected to dynamic loading	0.33	0.29	0.89	0.42	3.16	0.25
D	Components 1 with enhanced connections subjected to dynamic loading	0.89	0.25	1.75	0.41	<sup>(1)</sup>	<sup>(1)</sup>
E	Components 2 with basic connections subjected to quasi-static loading	0.78	0.35	1.18	0.28	1.44	0.39
F	Components 2 with enhanced connections subjected to quasi-static loading	0.70	0.39	1.01	0.25	1.20	0.29
G	Components 3 with basic connections subjected to dynamic loading	0.33	0.26	1.17	0.25	3.74	0.25
H	Components 3 with enhanced connections subjected to dynamic loading	1.11	0.25	2.81	0.32	4.54	0.25

<sup>(1)</sup> DS was not triggered

**Table 10.** Probabilities of exceedance of the defined DSs for the Eurocode 8 limits

Component Group	Description	DS1		DS2		DS3	
		0.75%	1.00%	0.75%	1.00%	0.75%	1.00%
A	Components 1 with basic connections subjected to quasi-static loading	0.94	0.98	0.11	0.46	<b>0.00</b>	0.09
B	Components 1 with enhanced connections subjected to quasi-static loading	<b>0.03</b>	0.21	<b>0.00</b>	0.07	<b>0.00</b>	<b>0.00</b>
C	Components 1 with basic connections subjected to dynamic loading	1.00	1.00	0.36	0.62	<b>0.00</b>	<b>0.00</b>
D	Components 1 with enhanced connections subjected to dynamic loading	0.26	0.69	<b>0.01</b>	<b>0.05</b>	<sup>(1)</sup>	<sup>(1)</sup>
E	Components 2 with basic connections subjected to quasi-static loading	0.75	0.95	<b>0.00</b>	0.16	<b>0.00</b>	<b>0.00</b>
F	Components 2 with enhanced connections subjected to quasi-static loading	0.96	1.00	0.13	0.50	<b>0.00</b>	<b>0.07</b>
G	Components 3 with basic connections subjected to dynamic loading	1.00	1.00	<b>0.04</b>	0.27	<b>0.00</b>	<b>0.00</b>
H	Components 3 with enhanced connections subjected to dynamic loading	0.06	0.34	0.00	<b>0.00</b>	<b>0.00</b>	<b>0.00</b>

<sup>(1)</sup> DS was not triggered.

The main fragility parameters, i.e., median values and standard deviations of the lognormal distributions, are compared with the results of selected past experimental studies. The considered researches are Retamales et al. [30] and Petrone et al. [31]. In particular, Retamales et al. carried out an experimental campaign for evaluating the seismic response, failure mechanisms, and fragilities of gypsum sheathed LWS partitions at the University of Buffalo. Specifically, twenty-eight in-plane quasi-static tests and 8 dynamic tests were carried out on 50 specimens (3.66 m long  $\times$  3.50 m high) connected at their ends to return partition walls (1.20 m long  $\times$  3.50 m high). However, only some Component Group were selected by [30] for the comparison with the research illustrated in this paper. Petrone et al. executed at the University of Naples six in-plane quasi-static tests on 5.00 m high gypsum sheathed LWS partitions. The main fragility parameters collected by the above-mentioned studies are listed in Table 11. The comparison highlights that the median values of the lognormal distribution experienced in this study for the Component Group A and for DS1 and DS2 (0.37% and 1.05%, respectively) are greater than the values defined in Petrone et al. (0.28% for DS1 and 0.81% for DS2). On the contrary, Petrone et al. recorded 2.05% as median value for DS3, which is greater

than the value given in this study (1.49%). The examination of test results for Component Group E and F highlights that the obtained median values (for Component Group E: 0.78% 1.18% and 1.44% for DS1, DS2 and DS3, respectively; for Component Group F: 0.70%, 1.01% and 1.20% for DS1, DS2 and DS3, respectively) are greater than the values obtained by Retamales et al. (for Component Group E: 0.27%, 0.61% and 1.20% for DS1, DS2 and DS3, respectively; for Component Group F: 0.26%, 0.68% and 0.75% for DS1, DS2 and DS3, respectively). Furthermore, the current study reveals a low statistical dispersion of the results with values of the standard deviation (from 0.25 to 0.51) lower than the values recorded in the other studies (from 0.33 to 0.59).

**Table 11.** Comparison between the main fragility parameters of different experimental studies

Authors	Component group	DS1		DS2		DS3	
		$x_m$ [%]	$\beta$ [-]	$x_m$ [%]	$\beta$ [-]	$x_m$ [%]	$\beta$ [-]
Current study*	A	0.37	0.51	1.05	0.29	1.49	0.29
	E	0.78	0.35	1.18	0.28	1.44	0.39
	F	0.70	0.39	1.01	0.25	1.20	0.29
Petrone et al. [31]	A	0.28	0.39	0.81	0.42	2.05	0.46
Retamales et al. [30]	E <sup>(2)</sup>	0.27	0.45	0.61	0.42	1.20	0.59
	F <sup>(3)</sup>	0.26	0.45	0.68	0.33	0.75	0.36

<sup>(1)</sup> DS was not triggered

<sup>(2)</sup> the reference is the subgroup 1b

<sup>(3)</sup> the reference is the subgroup 1a

From the examination of the in-plane response, some design implications can be given: (1) partition-to-surrounding connections (basic or enhanced anti-earthquake connections) significantly affect the in-plane response and a lower stiffness and strength were recorded for enhanced connections compared to basic connections; (2) partition-to-surrounding connections also influence the in-plane response in term of seismic vulnerabilities, and enhanced connections showed a better behaviour for partitions (Components 1) and façades (Components 3), except for partitions with return walls (Components 2), for which basic connection revealed a better seismic response; (3) the stud spacing (300 or 600 mm) does not influence the in-plane response; (4) façades have lower seismic vulnerabilities than partitions; (5) the IDR limits provided by Eurocode 8 Part 1, i.e. 0.75 and 1.00%, have been attributed to three groups of components and components with high (with an IDR limit of 0.75% for DS3), intermediate (with an IDR limits of 0.75 and 1.00% for DS2 and DS3) and low (with an IDR limit of 1.00% for DS2) seismic fragility have been identified.

## 7. CONCLUSIONS

An extended experimental research was performed at the University of Naples Federico II with the main goal to characterize the seismic behaviour of architectural non-structural LWS drywall

components, i.e. partitions, façades and ceilings. In particular, four architectural non-structural Components were identified: (1) Component 1, in which the partition was infilled in the surrounding structure and enclosed by structural elements on all sides (i.e. floors or beams and columns); (2) Component 2, in which the partition was enclosed by structural elements at the top and bottom (i.e. floors or beams) and connected at its ends to transversal façades (return walls); (3) Component 3, in which the façade was infilled in the surrounding structure and enclosed by structural elements on all sides (i.e. floors or beams and columns); (4) Component 4, in which the ceiling was suspended from the above floors and connected at the perimeter to partitions and façades. The Components were connected to the surrounding elements by means of two different typologies of partition or façade - to-surrounding connections: basic and enhanced anti-earthquake connections. The research was organized in three levels: ancillary tests, component tests and assembly tests.

As far as the out-of-plane behaviour of partitions (Components 1) is concerned, the main findings showed that the monotonic response in terms of strength and stiffness was strongly affected by stud spacing and their values doubled when spacing doubled (from 600 to 300 mm). Also the dynamic response in terms of damping ratio and fundamental vibration frequency was influenced by stud spacing, and 600 mm stud spacing partitions can be considered as flexible architectural non-structural components, whereas 300 mm stud spacing partitions showed a borderline behaviour between rigid and flexible components (according to ASCE/SEI 7-10). Considering the influence of partition-to-surrounding connections, the monotonic response of partitions was not affected by this parameter. However, the connection type influences the dynamic response of partitions and an increasing of damping ratio and a reduction of frequency were recorded when enhanced anti-earthquake connections were used, by highlighting a more flexible behaviour of enhanced connections compared to basic connections. EWM provides a good estimation of the out-of-plane strength of partitions, which could be schematized with simple supports at their ends, whereas the fundamental vibration frequency is underestimated with theoretical formulations. Furthermore, the out-of-plane dynamic response of partitions in terms of acceleration amplification was not affected by the connection type and partitions with both basic and enhanced connections showed values in the range from 1 to 2.

As far as the in-plane behaviour is concerned, results reveal that the responses of partitions (Components 1 and 2) and façades (Components 3) were not affected by stud spacing, whereas the partition or façade-to-surrounding connections played an important role on the seismic performance. In particular, basic connections provided additional strength and stiffness to the components starting from the initial phase of the response, whereas enhanced anti-earthquake connections provided additional strength and stiffness when the contact between sheathing boards and surrounding elements was restored. In fact, the enhanced anti-earthquake connections are interested by damages for inter-storey drift levels greater than basic-connections, by interacting with the surrounding

elements for higher inter-storey drift. Because the enhanced-connections had minor interaction with surrounding elements, they revealed a more flexible behaviour with higher values of the in-plane acceleration amplification (up to 4 and to 3 for partitions and façades, respectively) respect to basic connections (up to 2 for both partitions and façades). Furthermore, façades showed lower seismic vulnerabilities than partitions, because the DSs were triggered for higher median values of the lognormal distribution than those obtained for partitions. Finally, high, intermediate and low fragility components can be classified by taking into account the IDR limits provided by Eurocode 8 Part 1. In particular, an IDR of 0.75% can be considered an adequate limit for DS3 for high fragility components (Components 1 with basic connections and Component 2 with enhanced-connections), IDR limits ranging between 0.75 and 1.00% can be considered adequate limits for intermediate fragility components (Components 1 with enhanced connections and Components 2 and 3 with basic connections) and an IDR of 1.00% can be considered an adequate limit for the verifications of low fragility components (Component 3 with enhanced connections).

In conclusion, from the academic side, the results of the research project presented in this paper allow the advancement of the knowledge of the seismic performance of architectural non-structural LWS drywall components, opening the avenue for the improvement of the current seismic design provisions for non-structural components. From the industrial side, the characterization of the seismic performance of the most common European non-structural components represents an issue neglected until now and it provided the possibility to extend the market of non-structural components by improving the constructive details with the final aim to provide a better performance in seismic areas.

## **ACKNOWLEDGMENTS**

The study presented in this paper is a part of a wider research program coordinated by Prof. Raffaele Landolfo with the technical and financial support of Knauf Gips KG (research study agreement between Knauf Gips KG and the Department of Structures for Engineering and Architecture of the University of Naples “Federico II”, September 3, 2013). Knauf Gips KG is gratefully acknowledged by the authors for the Consent to Publish the scientific results presented in this paper in the scope of the above-mentioned common research.

## **REFERENCES**

- [1] American Society of Civil Engineers (ASCE), 2010. Minimum design loads for buildings and other structures, ASCE/SEI 7-10, Reston, VA.
- [2] American Society of Civil Engineers (ASCE), 2013. Seismic Evaluation and Upgrade of Existing Buildings. ASCE 41-13, Reston, VA.

- [3] European Committee for Standardization, (CEN), 2005. Eurocode 8—Design of Structures for Earthquake Resistance—Part 1: General Rules, Seismic Actions and Rules for Buildings, EN 1998- 1. Brussels, Belgium.
- [4] Ariyanayagam, A.D., Mahendran, M., 2018. Experimental study of non-load bearing light gauge steel framed walls in fire. *Journal of Constructional Steel Research* **145**:529-551.
- [5] Thanasoulas, I.D., Vardakoulias, I.K., Kolaitis, D.I., Gantes, C.J. and Founti, M.A., 2018. Coupled Thermo-Mechanical Simulation for the Performance-based Fire Design of CFS Drywall Systems. *Journal of Constructional Steel Research* **145**:196-209.
- [6] Mastrogiuseppe, S., Rogers, C.A., Tremblay, R., Nedisan, C.D., 2008. Influence of non-structural components on roof diaphragm stiffness and fundamental periods of single-storey steel buildings. *Journal of Constructional Steel Research* **64**(2):214-227.
- [7] Fang, M.J., Wang, J.F., Li, G.Q., 2013. Shaking table test of steel frame with ALC external wall panels. *Journal of Constructional Steel Research* **80**:278-286.
- [8] Li, Z., He, M., Wang, X., Li, M., 2018. Seismic performance assessment of steel frame infilled with prefabricated wood shear walls. *Journal of Constructional Steel Research* **140**:62-73.
- [9] Macillo, V., Fiorino, L., Landolfo, R. 2017. Seismic response of CFS shear walls sheathed with nailed gypsum panels: Experimental tests. *Thin-Walled Structures*, Elsevier Science. ISSN 0263-8231, **120**:161-171. doi: 10.1016/j.tws.2017.08.022
- [10] Fiorino, L., Shakeel, S. Macillo, V., Landolfo, R. 2018. Seismic response of CFS shear walls sheathed with nailed gypsum panels: Numerical modelling. *Thin-Walled Structures*, Elsevier Science, **122**:359-370. doi: 10.1016/j.tws.2017.10.028
- [11] Fiorino, L. Macillo, V., Landolfo, R. 2017. Shake table tests of a full-scale two-story sheathing-braced cold-formed steel building. *Engineering Structures*, Elsevier Science. ISSN 0141-0296, **151**:633–647. doi: 10.1016/j.engstruct.2017.08.056.
- [12] Fiorino, L., Macillo, V., Mazzolani, F.M., 2014. Mechanical behaviour of bolt-channel joining technology for aluminium structures, *Construction and Building Materials* **73**:76-88
- [13] Ye, J., Wang, X., Zhao, M., 2016. Experimental study on shear behavior of screw connections in CFS sheathing. *Journal of Constructional Steel Research* **121**:1-12.
- [14] Koliou, M., Filiatrault, A., 2017. Development of wood and steel diaphragm hysteretic connector database for performance-based earthquake engineering. *Bulletin of Earthquake Engineering* **15**(10): 4319–4347.

- [15] Nikolaidou, V., Latreille, P., Rogers, C.A., Lignos, D.G., 2017. Characterization of cold-formed steel framed / wood sheathed floor and roof diaphragm structures, in Proceedings of 16th World Conference of Earthquake Engineering, 09-13 January, 2017, Santiago, Chile.
- [16] Peterman, K.D. and Schafer, B.W., 2014. Sheathed cold-formed steel studs under axial and lateral load. *Journal of Structural Engineering* **140**(10).
- [17] Peterman, K., Benjamin, S., 2012. Stability of sheathed cold-formed steel studs under axial load and bending, in Proceedings of Structural Stability Research Council Annual Stability Conference, 18-21 April, 2012, Grapevine, Texas, USA, pp. 368-386.
- [18] Fiorino, L., Pali, T., Bucciero, B., Macillo, V., Terracciano, M.T., Landolfo, R., 2017. Experimental study on screwed connections for sheathed CFS structures with gypsum or cement based panels. *Thin- Walled Structures* **116**:234-249.
- [19] Rahmanishamsi, E., Soroushian, S., Maragakis, M., 2015. Cyclic shear behaviour of gypsum board-to-steel stud screw connections in non-structural walls. *Earthquake spectra* **32**(1):415-439.
- [20] Swensen, S., Deierlein, G.G., Miranda, E., 2016. Behavior of screw and adhesive connections to gypsum wallboard in wood and cold-formed steel-framed wallties. *Journal of Structural Engineering* **142**(4):E4015002.
- [21] Rahmanishamsi, E., Soroushian, S., Maragakis, M., 2016. Evaluation of the out-of-plane behaviour of stud-to-track connections in non-structural partition walls. *Thin-Walled Structures* **103**:221-224.
- [22] Freeman, S.A., 1977. Racking tests of high-rise building partitions. *Journal of the Structural Division* **103**(8):1673-1685.
- [23] Lee, T.H., Kato, M., Matsumiya, T., Suita, K., Nakashima, M., 2006. Seismic performance evaluation of non-structural components: drywall partitions. *Earthquake Engineering & Structural Dynamics* **36**(3):367-382.
- [24] Memari, A.M, Kasal, B., Manbeck, H.B., Adams, A.R., 2008. Experimental cyclic racking evaluation of light-frame wood stud and steel stud wall systems, PHRC Research Series Report No. 107, The Pennsylvania Housing Research Center, University Park, Pennsylvania, PA.
- [25] Restrepo, J.I., Bersofsky, A.M., 2011. Performance characteristics of light gage steel stud partition walls. *Thin-Walled Structures* **49**(2):317–324.
- [26] Restrepo, J.I., Lang, A.F., 2011. Study of loading protocols in light-gauge stud partition walls. *Earthquake Spectra* **27**(4):1169-1185.
- [27] Peck, Q., Rogers, N., Serrette, R., 2012. Cold-formed steel framed gypsum shear walls: In-plane response. *Journal of Structural Engineering* **138**(7):932-941.

- [28] Araya-Letelier G., Miranda E., 2012. Novel sliding/frictional connections for improved seismic performance of gypsum wallboard partitions, in Proceedings of 15<sup>th</sup> World Conference on Earthquake Engineering, 24-28 September, 2012, Lisboa, Portugal.
- [29] Tasligedik, A.S., Pampanin, S., Palermo, A., 2012. In-plane cyclic testing of non-structural drywalls infilled within RC frames, in Proceedings of 15<sup>th</sup> World Conference on Earthquake Engineering, 24-28 September, 2012, Lisboa, Portugal.
- [30] Retamales, R., Davies, R., Mosqueda, G., Filiatrault, A., 2013. Experimental seismic fragility of cold-formed steel framed gypsum partition walls. *Journal of Structural Engineering* **139**(8):1285–1293.
- [31] Petrone, C., Magliulo, G., Lopez, P., Manfredi, G., 2015. Seismic fragility of plasterboard partitions via in-plane quasi-static tests. *Earthquake Engineering & Structural Dynamics* **44**(14):2589-2606.
- [32] Swensen, S., Deierlein, G.G., Miranda, E., 2016. Behavior of screw and adhesive connections to gypsum wallboard in wood and cold-formed steel-framed wall-joints. *Journal of Structural Engineering* **142**(4):E4015002.
- [33] Amer, S., Hamoush, S., Abu-Lebdeh, T., 2016. In-plane performance of gypsum board partition wall systems subjected to cyclic loadings. *Journal of Constructional Steel Research* **124**:23-36.
- [34] Pali, T., Macillo, V., Terracciano, M.T., Bucciero, B., Fiorino, L., Landolfo, R., 2018. “In-plane quasi-static cyclic tests of non-structural lightweight steel drywall partitions for seismic performance evaluation”. *Earthquake Engineering & Structural Dynamics* **47**(6):1566-1588.
- [35] Davies, R.D., Retamales, R., Mosqueda, G., Filiatrault, A., 2011. Experimental Seismic Evaluation, Model Parameterization, and Effects of Cold-Formed Steel Framed Gypsum Partition Walls on the Seismic Performance of an Essential Facility, Technical Report MCEER 2011-0005, MCEER, State University of New York at Buffalo, New York.
- [36] Fiorino, L., Pali, T., Landolfo, R., 2018. Out-of-plane seismic design by testing of non-structural lightweight steel drywall partition walls. *Thin-Walled Structures* **130**:213-230.
- [37] McCormick, J., Matsuoka, Y., Pan, P., 2008. Evaluation of non-structural partition walls and suspended ceiling systems through a shake table study, in Proceedings of Structures Congress 2008, April 24-26, 2008, Vancouver, British Columbia, Canada.
- [38] Matsuoka, Y., Suita, K., Yamada, S., Shimada, Y., Akazawa, M., 2008. Non-structural component performance in 4-story frame tested to collapse, in Proceedings of the 14<sup>th</sup> World Conference on Earthquake Engineering, October 12-17, 2008, Beijing, China.

- [39] Magliulo, G., Petrone, C., Capozzi, V., Maddaloni, G., Lopez, P., Manfredi, G., 2014. Seismic performance evaluation of plasterboard partitions via shake table tests. *Bulletin of Earthquake Engineering* **12**(4):1657-1677.
- [40] Wang, X., Pantoli, E., Hutchinson, T.C., Restrepo, J.I., Wood, R.L., Hoehler, M.S., Grzesik, P., Sesma F.H., 2015. Seismic performance of cold-formed steel wall systems in a full-scale building. *Journal of Structural Engineering* **141**(10):04015014.
- [41] Chen, M.C., Pantoli, E., Wang, X., Astroza, R., Ebrahimian, H., Hutchinson, T.C., Conte, J.P., Restrepo, J.I., Marin, C., Walsh, K.D., Bachman, R.E., Hoehler, M.S., Englekirk, R., Faghihi, M., 2016. Full-scale structural and non-structural building system performance during earthquakes: Part I – specimen description, test protocol, and structural response. *Earthquake Spectra* **32**(2):737–770.
- [42] Pantoli, E., Chen, M.C., Wang, X., Astroza, R., Ebrahimian, H., Hutchinson, T.C., Conte, J.P., Restrepo, J.I., Marin, C., Walsh, K.D., Bachman, R.E., Hoehler, M.S., Englekirk, R., Faghihi, M., 2016. Full-scale structural and non-structural building system performance during earthquakes: Part II – NCS damage states. *Earthquake Spectra* **32**(2):771–794.
- [43] Jenkins, C., Soroushian, S., Rahmanishamsi, E., Maragakis, E.M., 2016. Experimental fragility analysis of cold-formed steel-framed partition wall systems. *Thin-Walled Structures* **103**:115-127.
- [44] Petrone, C., Magliulo, G., Manfredi, G., 2017. Shake table tests on standard and innovative temporary partition walls. *Earthquake Engineering & Structural Dynamics*, **46**(10):1599-1624.
- [45] Bucciero, B., Pali, T., Terracciano, M.T., Macillo, V., Fiorino, L., Landolfo, R., 2018. Shake Table Testing of Lightweight Steel Drywall Non-structural Components., in *Proceedings of the 9th International Conference on Behaviour of Steel Structures in Seismic Areas (STESSA 2018)*. Christchurch, New Zealand. Mazzolani F.M., MacRae G., Clifton C., Key Engineering Materials, ISSN: 1662-9795, **763**: 423-431, doi:10.4028/www.scientific.net/KEM.763.423.
- [46] European Committee for Standardization, (CEN), 2006. Eurocode 3—Design of Steel Structures—Part 1-3: General Rules—Supplementary Rules for Cold-Formed Members and Sheeting, EN 1993-1-3. Brussels, Belgium.
- [47] European Committee for Standardization, (CEN), 2009. Continuously Hot- Dip Coated Steel Flat Products—Technical Delivery Conditions, EN 10346. Brussels, Belgium.
- [48] Ramasco, R. (1993). *Dinamica delle strutture*, CUEN.
- [49] American Iron and Steel Institute (AISI), 2016. North American Specification for the Design of Cold-Formed Steel Structural Members, AISI-S100-16. Washington, D.C.

- [50] Federal Emergency Management Agency (FEMA), 2007. Interim testing protocols for determining the seismic performance characteristics of structural and non-structural components, FEMA 461, Washington, D.C.
- [51] International Conference of Building Officials Evaluation Service (ICBO), 2000. Acceptance criteria for the seismic qualification of non-structural components, ICBO-AC156. Whittier, CA.
- [52] Porter, K., Kennedy, R., Bachman, R., 2007. Creating fragility functions for performance-based earthquake engineering. *Earthquake Spectra* **23**(2):471- 489.
- [53] Lilliefors, H., 1967. On the Kolmogorov-Smirnov test for normality with mean and variance unknown. *Journal of the American Statistical Association* **62**(318):399- 402.